공학석사 학위논문

Collision Risk Analysis of a Satellite with Fragments from Break-up of a Space Object

분열된 우주물체의 파편들에 대한 인공위성의 충돌위험 분석

2022년 12월

서울대학교 대학원

협동과정 우주시스템전공

윤 정 훈

Collision Risk Analysis of a Satellite with Fragments from Break-up of a Space Object

분열된 우주물체의 파편들에 대한 인공위성의 충돌위험 분석

지도교수 이 복 직

이 논문을 공학석사 학위논문으로 제출함

2022년 12월

서울대학교 대학원

협동과정 우주시스템전공

윤 정 훈

윤정훈의 공학석사 학위논문을 인준함

2022년 12월

위 원 장 _____ (인)

부위원장 _____ (인)

위 원 _____ (인)

Abstract

Collision Risk Analysis of a Satellite with Fragments from Break-up of a Space Object

Jeonghoon Yun
Interdisciplinary Program in Space Systems
The Graduate School
Seoul National University

Recently, with the rise of a New Space era, the initiative in space development is gradually shifting to the private sector. Accordingly, satellites are manufactured smaller, and the operation of constellations is gradually increasing. In contrast, as global interest in the use of the space domain grows, some powers are developing and testing ASAT weapons to compete for international supremacy. As a result, artificial space objects are increasing rapidly, and the possibility of collision between space objects is also increasing significantly. If a space object is broken by a collision, it creates numerous fragments that can pose a threat to other satellites.

In the present study, it is analyzed that the collision risk of fragments generated after a break-up of a space object with another satellite. And it was proposed that a three-step collision risk analysis model which can analyze collision risk. First, the NASA EVOLVE 4.0 breakup model was used to describe the fragments caused by the fragmentation of the space object. Second, the orbits of each generated fragment were propagated using a

numerical orbit model. Lastly, collision risk was analyzed by applying the probability of collision analysis method proposed by Patera.

To validate that our model works properly, case studies were conducted concerning the anti-satellite (ASAT) test for FY 1C in 2007 by China and ASAT test for COMSMOS 1408 in 2021 by Russia. In addition, a hypothetical case study was conducted to analyze the risk between ISS and fragments from the virtual break-up of KMS 4. Finally, a case study was conducted in which KMS 4 was intentionally broken before approaching the ISS, and an analysis was performed on the point at which the maximum collision probability appeared.

As a result of the study, the model of the present study describes the fragments of the broken space object similarly, and the risk analysis could be properly performed. Moreover, It was possible to know the effective time for indirect satellite attacks through fragments of a broken space object

Using the present study, satellite operators may be able to prepare for the situation of the break-up of space objects in the space domain. And it is also expected that the R.O.K. Armed Force will not only improve its ability in space domain awareness but also improve its operational capabilities in the space domain, which may become a new battlefield.

Keyword : NASA EVOLVE 4.0 breakup model, Patera's method, Space fragments, Satellites, Miss-distance, Probability of Collision
Student Number : 2021-28391

Table of Contents

Tables

Figures

1. Introduction

1.1 Background

Since the launch of Sputnik 1 in 1957, mankind has launched satellites into space for various purposes for 65 years. Recently, demand for satellite data has been increasing in various fields such as commercial and military. In response, numerous countries have begun to develop the space industry through satellites, and the number of satellites in space is rapidly increasing.

Recently, according to the trend of space development in the New Space era, the direction of satellite development is changing from multi-purpose and large satellites led by the state to single-purpose and small satellites led by the private. Accordingly, the paradigm of satellite operation has also turned single satellite operations into constellations. Constellation refers to a satellite group in which numerous satellites are clustered to perform a given mission.

Table 1. show the paradigm shift of space development. Notably, the paradigm is being altered to launch satellites more frequently instead of shortening the lifespan of satellites. Terefore, the number of satellites is expected to increase faster than now [1].

Table 1. Paradigm shift of satellite development

Old Space	New Space
Led by the government	led by the private
Multi-mission	A specific mission
Single Satellite	Constellation
long life span	short life span
Large satellite	Small Satellite
Low launch opportunity	High launch opportunity
High launch cost	low launch cost

As an example of this change, SpaceX's Starlink constellation have been launched more than 3,000 satellites into orbit [2], with 12,000 satellites to be deployed in the future, consequently, more satellites are expected to be launched in space than now. As can be seen from Fig. 1 and Fig.2, the Space Environment Report, published annually by the Space Debris Office in the European Space Agency (ESA), show that commercial satellite and constellations operating in low orbit have been increased significantly in 2022 [3].

However, the increase in the number of satellites can cause severe disasters such as mutual collisions between satellites. Due to the hypervelocity, the collision between satellites may result in fatal consequences such as space debris, which can interfere with satellite operators' stable satellite operations. Space debris means debris from space launch vehicles, ejected propellant, battery explosion of payload, rocket body explosions from the hypergolic propellant, abrupt mutual collision as well as Anti-satellite (ASAT) test [4].

If Space debris is generated, it is impossible to control, is difficult to track due to its small size and low mass, and maintains a hypervelocity, which could be disastrous when colliding with a satellite, so it would be a major threat to the satellite operations. Moreover, If space debris collides with a satellite, the satellite will be destroyed, resulting in another Space debris, which could lead a cascading chain reaction such as Kessler Syndrome [5]. If this situation occurs, mankind may not be able to use space, which can have a significant negative impact on human life. Therefore, internationally, all the countries are striving for the peaceful utilization of space and stable operation of satellites.

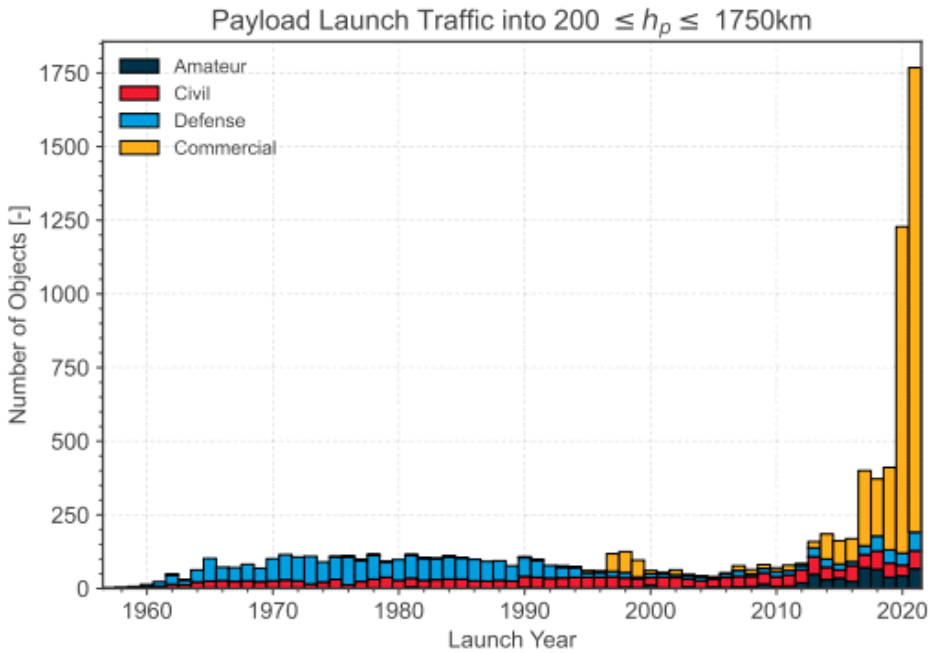

Fig. 1 Increasing commercial satellite at the New Space era [3]

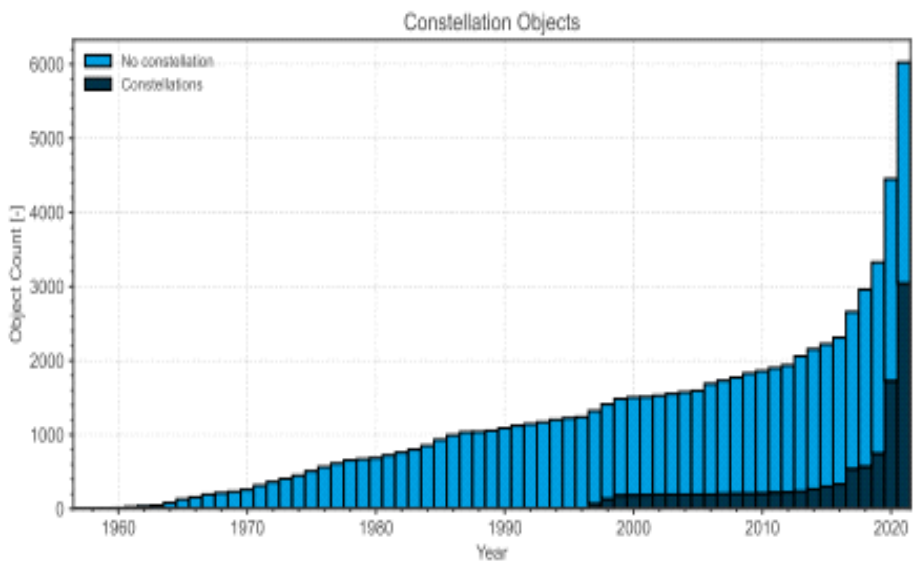

Fig. 2 Increasing number of Satellite Constellations [3]

However, during the Cold War, the competition for the development of space had been conducted by the U.S. and the Soviet Union, and the Soviet Union had manufactured satellites to self-destruct at the end of their lifespan to prevent a situation where their satellites and information were passed over to the U.S. also, the Soviet Union intentionally destructed their early warning satellites if they failed to enter planned orbit [6]. Furthermore, they conducted an ASAT test by intentionally colliding two satellites on earth orbit [4].

The U.S. also intercepted the Sowind P78-1 satellites through the ASAT test in 1985, and China conducted an ASAT test intercepting the meteorological satellite Fengyun1C(FY 1C) satellite with a ballistic missile in 2007, resulting in 3,000 space debris [4]. In addition, the U.S. communication satellite Iridium 33 and the Russian military satellite COSMOS 2251 unintentionally collided with each other, generating more than 1,600 fragments in 2009 [7,8]. The remnants of these series of events still interfere with the operation of satellites around the world even a few decades later.

1.2 Purpose of research

As mentioned earlier, the destruction of satellites due to ASAT tests, collisions, or explosions can produce numerous fragments that are difficult to predict. Therefore, various studies have been conducted in two branches to manage those situations.

First of all, research was conducted to predict the situation of satellite fragmentation. Especially, space agencies such as NASA and ESA have studied the characteristics of space debris, such as its eject velocity, mass, area, and fragment shape, and have developed a satellite breakup model, such as IMPACT, FREMAT,

and EVOLVE [9-14].

Secondly, research was conducted to analyze the probability of collision (POC) between space objects. Space agencies such as NASA, European Space Agency (ESA), France's National Space Research Center (CNES), Japan's Aerospace Research and Development Organization (JAXA), and Korea's Aerospace Research Institute (KARI) have been developing software that can evaluate the POC between satellites and establishing strategy of satellites evasion maneuver when POC reaches a certain rate [15]. And many researchers such as Foster [16], Chan [17-20], Patera [21-25], Alfano [26-28], Berend [29], Alfriend [30], Akella [31], Vedder [32] and Serra [33] suggested various methods to effectively analyze the POC.

The Republic of Korea Armed Forces is also entering space development and deploying various satellites. Especially Republic of Korea Armed Forces plans to launch hundreds of satellites into orbit in the near future. Therefore, it is necessary that the Republic of Korea Armed Forces should conduct researches that can predict the breakup of space objects and analyze the collision risk of impacting a satellite by generated fragments.

For this reason, to evaluate a satellite's POC from fragments of a broken space object, we combined the aforementioned research of two fields. we adopted NASA EVOLVE 4.0 breakup model among the satellite breakup models and the Patera method among POC analysis methods. Afterward, through case studies, analyses were conducted on the collision risk immediately after the satellite's breakup.

2. Method

2.1 Satellite Break-up Model

In the present study, we adopted the NASA EVOLVE 4.0 Breakup Model developed by NASA. In the early 1970s, NASA's Orbital Debris Program Office first developed a breakup model called EVOLVE to model space debris. EVOLVE was subsequently developed to EVOLVE 4.0 in 2000 by complementing data such as the destruction caused by the collision of Solwind P78-1 and the Satellite Orbital Debris Characterization Impact Test (SOCIT), and the explosion test on the top of ESA's Ariane rocket [13].

EVOLVE 4.0 is a model that organizes the distribution of characteristic length (Lc), area (A), mass (M), area-to-mass ratio (A/M), and ejection velocity of fragments. If input parameters such as mass and collision velocity of colliding objects and Lc are input to this model, fragments larger than input Lc are generated, and the number of fragments is determined by using power-law distribution. After that, the A/M distribution is mapped through the distribution of the generated Lc. Then, the mass and area of each fragment are obtained through the A/M distribution, and the corresponding ejection velocity is obtained [13].

However, since EVOLVE 4.0 relies on empirical data, it has limitations that do not fit physics such as mass conservation and momentum conservation. To address this problem, Joubert proposed a method to approximate the conservation of mass and momentum to overcome the physical limitations of EVOLVE 4.0 [14].

According to Joubert, to approximate the conservation of mass, as shown in Eq. (1), it was assumed that mass is conserved if the

sum of the masses of the fragments exceeds 60% of the mass of the object before impact. Also for momentum conservation, as shown in Eq. (2), it was suggested that momentum conservation is approximately achieved when the sum of the momentums of all fragments is less than 0.01 times the sum of the momentums of each fragment [14].

$$\sum_{i=1}^{n} m_i \geq 0.6 \times m_{target} \tag{1}$$

$$\left| \sum_{i=1}^{n} m_i \boldsymbol{v_i} \right| \leq \sum_{n=i}^{n} \left| m_i \boldsymbol{v_i} \right| \times 0.01 \tag{2}$$

In the present study, among the methods proposed by Joubert, the law of conservation of momentum was utilized as it is. However, for the law of conservation of mass, the existing law was used as shown in Eq. (3).

$$\sum_{i=1}^{n} m_i = m_{target} \tag{3}$$

Fig. 3 depicts a flow chart of the Breakup model used in this study. If the sum of the masses of the fragments is not equal to the mass of the object before the collision, this model adds or subtracts fragments to meet the mass conservation. And, to meet the momentum conservation, the ejection velocity of fragments is extracted again if Eq. (2). is not satisfied.

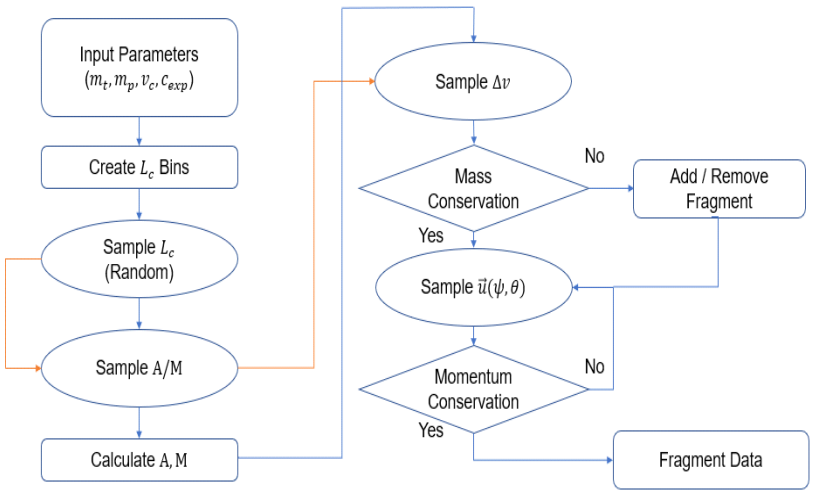

Fig. 3 Flow chart of generating fragments data

2.2 Orbit Propagation

In the present study, the ejection velocity vector of each fragment generated based on the break-up model was added to the original velocity vector of the satellite before the break-up, and then the position and velocity were propagated by numerical integration using Kepler's two-body equation.

To acquire the Cartesian coordinates of the satellite to be used for numerical orbit propagation, the Keplerian orbital elements (KOE) devised by Kepler must first be obtained. KOE can be obtained by using the Two Line Element (TLE) provided by the Celestrak homepage [2] operated by North American Aerospace Defense Command (NORAD). TLE is recorded as a series of numbers in two lines, which include data such as satellite identification number, generation time, KOE, drag parameter (B*), period, and revolution number.

However, TLE is made for analytical models such as SGP4, and errors exist because it uses the average value between observation points rather than the actual value at a specific point in time, and thus uses a unique coordinate system called True Equatorial Mean Equinox (TEME). However, we used the J2000 coordinate system, and it has some errors compared with the TEME coordinate system due to the difference in the direction of the vernal equinox and whether precession and nutation are applied. For this reason, if the state vector obtained from TLE is just used, errors will occur, so it should be converted from the TEME to the J2000 coordinate system [2,34].

As can be seen in Eq. (3), the obtained state vector is composed of a radial vector representing the distance from the center of the earth to the position of the satellite and a velocity vector representing the speed and direction at that point.

$$\vec{r}_{ECI} = \begin{bmatrix} r_x & r_y & r_z \end{bmatrix}_{ECI}^{T} \quad , \quad \vec{v}_{ECI} = \begin{bmatrix} v_x & v_y & v_z \end{bmatrix}_{ECI}^{T} \tag{4}$$

And then, after entering the initial state vector into the two-body equation as shown in Eq. (5), the radial and velocity vector up to the required epoch are propagated. In the present study, numerical integration is performed using Cowell's method, and RK4 Integrator based on the 4th order Runge-Kutta method was applied [34].

$$\vec{r} = -\frac{\mu}{r^2}\frac{\vec{r}}{r} \tag{5}$$

where μ is a gravitational constant in which value is $3.986 \times 10^5 \, (km^3/s^2)$, $\boldsymbol{r}$ is radial vector from center of the earth, $\ddot{\boldsymbol{r}}$ is a acceleration vector as the secondary differential term of $\boldsymbol{r}$, and r is scalar of $\boldsymbol{r}$.

In order to propagate a more precise orbit by using a numerical method, special perturbation should be considered with the two-body equation shown in Eq. (5). However, It is so hard to propagate all of the fragments' orbits due to its large number, so we considered only the two most affecting perturbation. The satellites covered in this study are mainly satellites in low earth orbit (LEO) within 2000 km. In that case, the perturbations that have the greatest effect on the motion of the satellite are effect and atmospheric drag. The effect refers to the perturbation caused by precession due to the oblateness of the Earth, and the atmospheric drag refers to the perturbation caused by the thin air layer of inner space. So, only these two perturbations were considered. So, the two perturbations added in the two-body equation as can be seen in Eq. (6), and through this, it was possible to not only propagate a more precise orbit of fragments but also reduce the computational cost.

$$\ddot{\vec{r}} = -\frac{\mu}{r^2}\frac{\vec{r}}{r} + F_{J2} + F_{Drag} \tag{6}$$

where, F_{J2} is perturbation of J_2 effect and it expressed as Eq. (7) below [35].

$$F_{J2} = \frac{3\mu J_2 R_e^2}{2r^5}\left[\left(5\frac{\vec{r} \cdot \vec{r_z}}{r^2} - 1\right)\vec{r} - 2(\vec{r} \cdot \vec{r_z})\vec{r_z}\right] \tag{7}$$

where, J_2 is constant with a value of 1.08263×10^{-3}, R_e is the Earth's radius, and $\vec{r_z}$ is the satellites z-axis vector.

F_{Drag} in Eq. (6) expressed as in Eq. (8) below [34].

$$F_{Drag} = -\frac{1}{2}\frac{C_D A}{m}\rho v_{rel}^2 \frac{\vec{v}_{rel}}{|\vec{v}_{rel}|} \tag{8}$$

where, C_D is the coefficient of drag, ρ is the atmospheric density at the altitude of the satellite, A is the cross-sectional area of the satellite and $\vec{v}_{rel}$ is the rotational angular velocity of the atmosphere due to the rotation of the earth and it can be expressed by the following equation Eq. (9) [34].

$$\vec{v}_{rel} = \frac{d\vec{r}}{dt} - \vec{\omega}_e \times \vec{r} = \left[\frac{dx}{dt} + \omega_e y \quad \frac{dy}{dt} + \omega_e x \quad \frac{dx}{dt}\right]^T \tag{9}$$

where, ω_e is the angular velocity of the rotation of the earth, and has a value of $7.292\times10^{-5}\,(rad/s)$.

In Eq. (9), the Earth's atmospheric density has a different value depending on the altitude. So much research on the atmospheric density model has been proposed so far, in this research, we use the MSIS atmospheric density model developed by Hedin in 1986 [36].

2.3. Probability of Collision

2.3.1 General Method

In general, to analyze the probability of collision, it is necessary to know the position closest approach (PCA) where each fragment is closest to the satellite, and the Time Closest Approach (TCA) when it reaches PCA, and they can be acquired by numerical orbit propagation. However, there are two errors in the prediction orbit obtained by the propagation model. The first error is the initial error caused by errors in TLE data, and the second is the model error caused by the orbit propagation model [37]. Because of this, the actual position of satellites and fragments differ from those propagated. In order to consider these errors, a satellite-based orbit coordinate system and a probability density function are usually used.

Usually, a satellite-based orbit coordinate system is obtained based on the flight direction of the satellite (In-track) or the direction from the center of the earth to the satellite (Radial). The former is an UVW coordinate system and the latter is an RSW coordinate system. In this study, we use the former coordinate system. In any of the two coordinate systems, each axis has a position error that is a sum of the initial error and the model error. And then, an error ellipsoid having each axis position error as radii is generated. At this error ellipsoid, the position error value for each axis can be regarded as the standard deviation of the probability density function, and through this, error covariance can be obtained [26,34].

When the error ellipsoids of two objects meet or overlap each other, it can be seen as a space where there is a high probability that two objects can collide, and when the two objects come into

contact, it can be seen that a collision occurs. Therefore, the POC can be obtained by integrating the sum of the volume of each object at the position where each object contacts in a three-dimensional probability density function. And, when calculating the sum of the volumes of two objects, we assume each object is a sphere and create a combined sphere with the sum of the radii of each object. After that, by integrating the volume of the combined sphere in the 3-dimensional probability density function, POC can be obtained by solving Eq. (10) [21,25,28,34].

$$POC = \frac{1}{\sqrt{8\pi^3}\sigma_x\sigma_y\sigma_z} \iiint_V \exp\left[\frac{-x^2}{2\sigma_x^2} + \frac{-y^2}{2\sigma_y^2} + \frac{-z^2}{2\sigma_z^2}\right] dxdydz \tag{10}$$

In this study, when we calculated POC, the model error was not considered assuming that the orbit propagation model is precise, but only the initial error obtained by TLE was considered. As shown in Table 2, the initial error was obtained using the mean error of TLE by altitude proposed by ESA [38,39].

Table 2. Mean orbit error of TLE catalog analyzed by ESA [38,39]

Orbit regime	Averaged σ_U [km]	Averaged σ_V [km]	Averaged σ_W [km]
LEO	0.102	0.471	0.126
MEO	0.073	0.131	0.054
GTO	1.960	3.897	1.808
HEO	0.824	1.367	1.059
GEO	0.359	0.432	0.086

2.3.2 Patera's Method

The method described above is a general method for obtaining the collision probability, but the calculation is complicated, such as performing the integration three times. Moreover, since numerous fragments of broken satellites have to be analyzed, calculations are needed as simply as possible. For this reason, we use Patera's method which is computationally fast and suitable for multiple POC analyses [21,22,40].

Patera simplified the general POC analysis from the 3-D integration problem to the 1-D contour integration problem through a series of processes. In Patera's method, the combined covariance and combined sphere in TCA are projected into a two-dimensional encounter plane. In this encounter plane, the relative position between two objects is the crucial parameter. Set the center of the projected combined covariance as the coordinate origin, and place the center of the projected combined sphere at the end of the relative position vector. In this process, the projected combined sphere is called hard body, and the 2-D integration of the area of the hard body in the encounter plane becomes the POC.

After that, Patera rotated the two-dimensional axes using a rotational matrix so that the major and minor axes of the error covariance ellipse heading for each axis, and adjusted the size of one of the two axes to transform the probability density function of each axis to be symmetric. As a result, the position vector and shape of the hard body change. Finally, By converting a two-dimensional cartesian coordinate system into a polar coordinate system, Patera transformed the integration problem for the area of the hard body into a path integration problem for the perimeter of the hard body as shown in Eq. (11) and Eq. (12) [21].

$$POC = -\frac{1}{2\pi}\oint_{\ell ipse} \exp(-\alpha r^2)d\theta \tag{11}$$

where, α is a scale factor of the x-axis after the rotation of the coordinate system, r is the distance from the origin of the polar system to points around the hard body, and θ is the rotational angle of the x-axis.

$$POC = 1 - \frac{1}{2\pi}\oint_{\ell ipse} \exp(-\alpha r^2)d\theta \tag{12}$$

And if the distance between the centers of the two objects is less than the sum of the radii of the two objects, Eq. (11) is replaced by Eq. (12).

2.3.3 Numerical Integration of Patera's Method

To perform numerical integration for Patera's POC method Eq. (11) and Eq. (12), the state vector above the hard body perimeter must be obtained first, and the vector of the hard body center and the entire perimeter of the hard body are required. To do this, we first define a unit circle with a radius value of one, and select the point $\boldsymbol{X}$ = (1, 0) on that unit circle. And to define $\boldsymbol{X}'$ close to $\boldsymbol{X}$, $\boldsymbol{X}$ is multiplied by the rotational matrix R of the angle ϵ.

$$\boldsymbol{X}' = R\boldsymbol{X} \tag{13}$$

$$R = \begin{bmatrix} \cos(\epsilon) & -\sin(\epsilon) \\ \sin(\epsilon) & \cos(\epsilon) \end{bmatrix} \tag{14}$$

Then, to make the identical shape as the hard body, each vector is multiplied by the matrix M reflecting the scale-factor.

$$\boldsymbol{X}'_m = M\boldsymbol{X}', \quad \boldsymbol{X}_m = M\boldsymbol{X} \tag{15}$$

$$M = \begin{bmatrix} s & 0 \\ 0 & s\sqrt{\beta/\alpha} \end{bmatrix} \tag{16}$$

The relative distance vector of the two objects os then added to each vector, where the X component of each vector is added to the X component of the initial relative distance vector q_x, and the Y component of each vector is added to the Y component of the scale-adjusted relative distance vector q_{ys}.

$$\boldsymbol{X}_e = \boldsymbol{X}_m + \begin{bmatrix} q_x \\ q_{ys} \end{bmatrix}, \quad \boldsymbol{X}'_e = \boldsymbol{X}'_m + \begin{bmatrix} q_x \\ q_{ys} \end{bmatrix} \tag{17}$$

Thereafter, the angle between the two vectors can be obtained as shown in Eq. (18) and Eq. (19) using the characteristics of the cross product of the vector.

$$\boldsymbol{X}_e \times \boldsymbol{X}_e' = |\boldsymbol{X}_e||\boldsymbol{X}_e'|\sin(d\theta) \tag{18}$$

$$d\theta = \sin^{-1}\frac{\boldsymbol{X}_e \times \boldsymbol{X}_e'}{|\boldsymbol{X}_e||\boldsymbol{X}_e'|} \tag{19}$$

The integrand I_n can be expressed as an equation for the intermediate value of the two vectors as shown in Eq. (20).

$$I_n = \exp[-\alpha(\frac{\boldsymbol{X}_e + \boldsymbol{X}_e'}{2})^2] \tag{20}$$

The POC is obtained by summering the product of I_n and $d\theta_n$ for each interval of the perimeter divided by N intervals like Eq. (21) and Eq (22).

$$POC = -\frac{1}{2\pi}\sum_{n=1}^{N} I_n d\theta_n \tag{21}$$

when origin is excluded from hard body,

$$POC = 1-\frac{1}{2\pi}\sum_{n=1}^{N} I_n d\theta_n \tag{22}$$

when origin is included in hard body,

3. Verification of Model

In this study, verification of the model presented in chapter 2 was carried out to conduct case studies. Verification was carried out for each of the three steps of the collision probability analysis model used in this study. For the verification of the Satellite Breakup Model, the collision of COSMOS 2251 and iridium 33 that occurred in 2009 was used. And to verify orbit propagation model, To verify the orbit propagation model, it was checked whether the perturbations were applied properly, and the change in the orbital elements depending on whether J_2 effect and drag were applied was verified. Finally, To verify Patera's method, the result of SOCRATES [2], which is a POC analysis tool used by Celestrak was compared against the result of Patera's method.

3.1 Satellite Breakup Model

To verify that the fragments were properly generated, we used the A/M distribution diagram and Gabbard Diagram of each fragment. The A/M is a major determinant of mass, area, and ejection velocity in NASA's EVOLVE 4.0 breakup model. The Gabbard Diagram is a diagram showing the apogee and perigee of space objects orbiting the Earth on the axes of the period (x-axis) and the altitude (y-axis). This diagram shows the shape of each generated fragment orbit, and it is possible to know the altitude change of each fragment after break-up.

In the present study, we compared the A/M and Gabbard Diagram of the fragments generated by the break-up model with the actual data of each fragment cataloged after the collision of the Iridium 33 and the COSMOS 2251.

In the comparison of A/M distribution, the number of fragments generated in our model and that of cataloged was different, so the relative number of fragments was compared. As can be seen in Fig. 4 and Fig. 5, the A/M distribution of fragments of Iridium 33 and COSMOS 2251 appeared similar to that of the catalog.

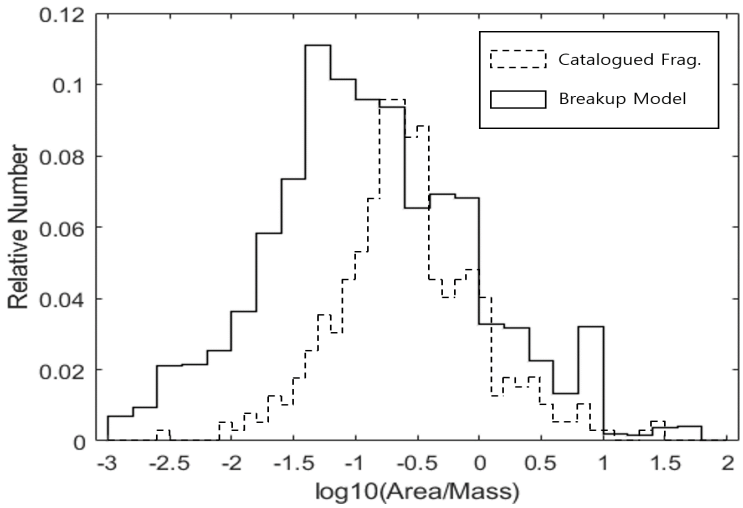

Fig. 4 A/M ratio distribution of Iridium 33

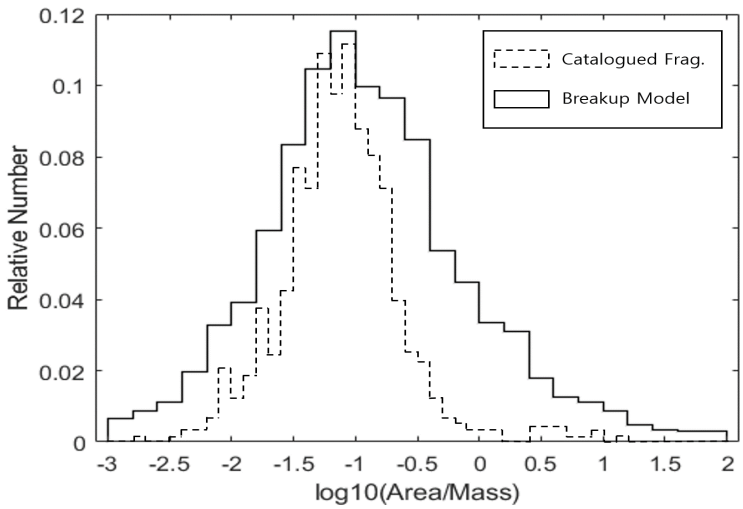

Fig. 5 A/M ratio distribution of COSMOS 2251

Fig. 6 and Fig. 7 show the Gabbard diagram showing catalog fragment data of Iridium 33 and COSMOS 2251 and that of generated by the breakup model.

It can be seen that they are gathered around the point of altitude of 779 km which is the break-up point, and the point of a period of 100.4 and 100.6 minutes, and the overall distribution is similar to each other.

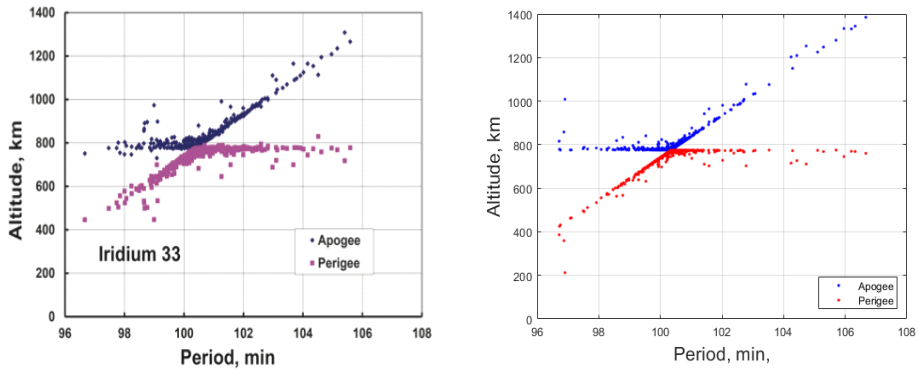

(a) Catalog (b) Breakup Model

Fig. 6 Comparison of breakup model and catalog of Iridium 33

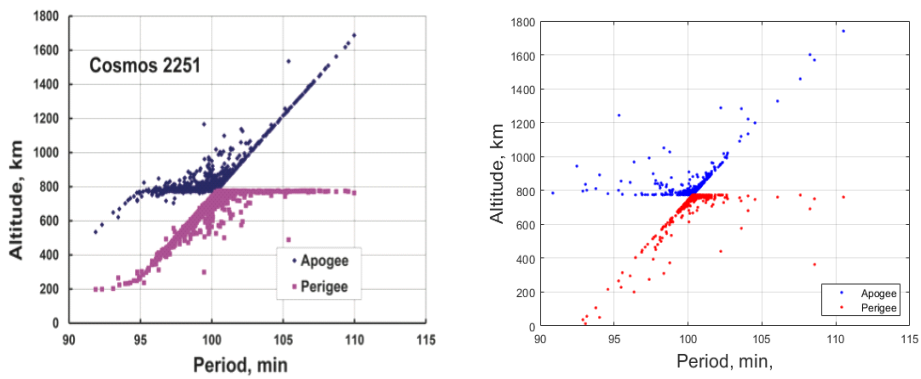

(a) Catalog (b) Breakup Model

Fig. 7 Comparison of breakup model and catalog of COSMOS 2251

3.2 Orbit Propagation

In the verification of the orbit propagation model, we verified whether the perturbation term is applied properly. The KMS 4 satellite operated by North Korea was selected as the target of orbital propagation, and the application of J_2 effect and drag was verified.

Fig. 8 shows the changes in the argument of perigee (ω) and the Right Ascension of Ascending Node (Ω) during the 24 hours according to the addition of the perturbation term of J_2 effect. In the above Fig. 8, ω and Ω were constant that values are 395.78° and 335.4° each. After adding J_2 perturbation, ω vibrated between 280° and 80°, and Ω was increased about 1° from 335.4° to 336.4°.

Through these results, it was verified that the vibration of ω and the change of Ω, which are the effects of J_2, were reflected properly. Especially in the case of the change of Ω, the characteristic of KMS 4, which changes 1° per day while orbiting the Sun Synchronous Orbit (SSO), was reflected very close.

Fig. 9 shows the changes in altitude (H) and semi-major axis (a) for a week depending on whether or not atmospheric drag was reflected. As a result of the verification, before adding atmospheric drag perturbation, the altitude is constantly vibrated between a minimum of 410 km and a maximum of 434 km, and the semi-major axis was kept constant. However, after adding that, the minimum altitude decreased from 419 km to 418 km, and the maximum altitude also decreased from 434 km to 433 km, indicating a decrease in altitude of about 1 km. Also, the semi-major axis vibrated between 6788 km and 6808 km. It means atmospheric drag perturbation was reflected properly.

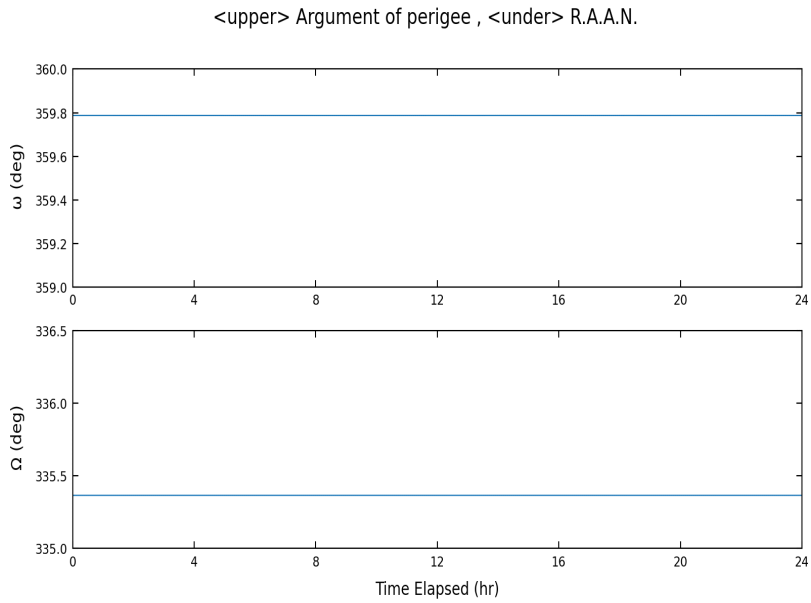

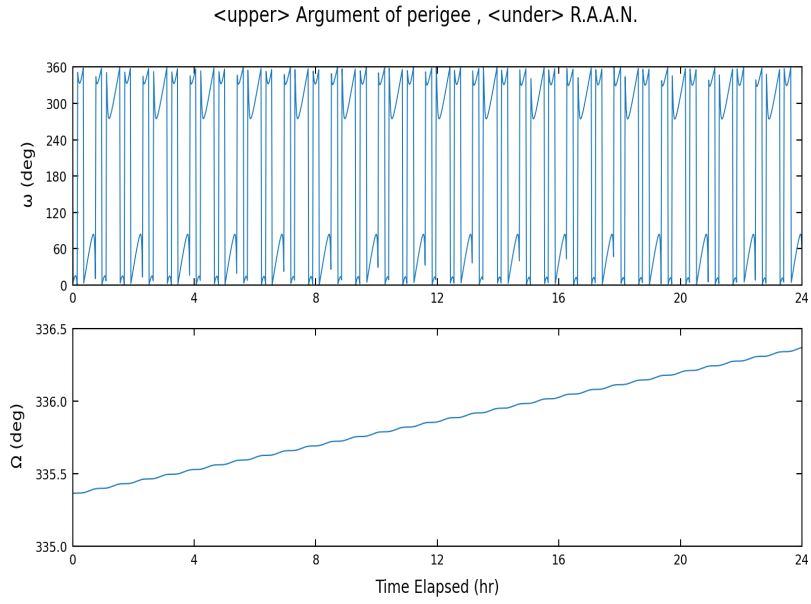

Fig. 8 Change of ω and Ω of KMS 4 due to J_2 effect

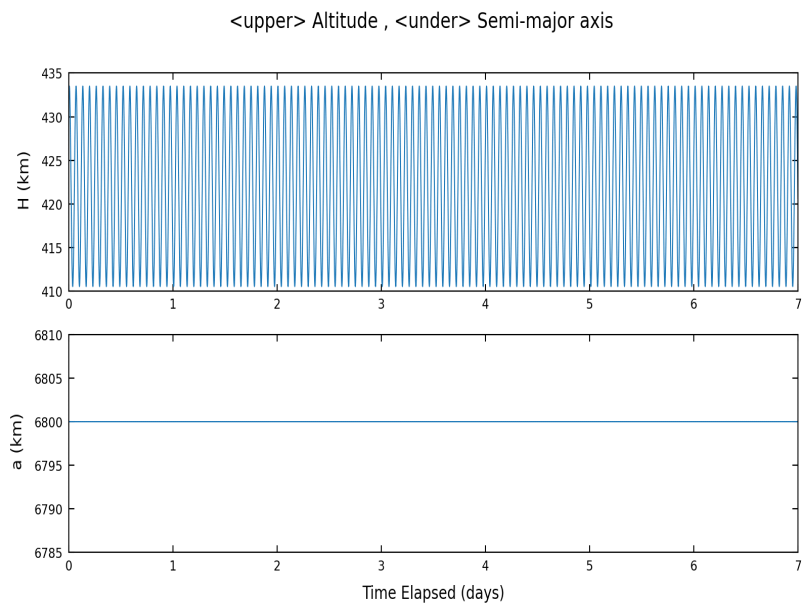

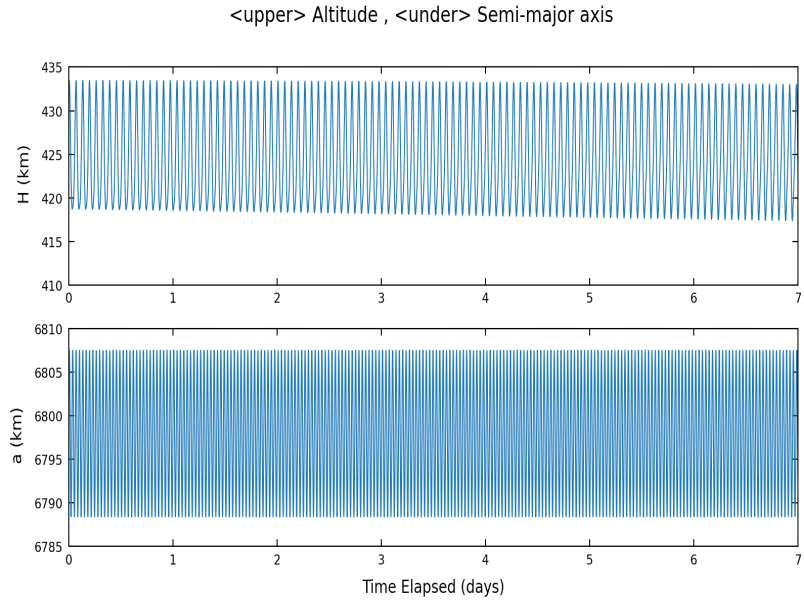

Fig. 9 Change of altitude and semi-major axis of KMS 4 due to drag

3.3 Patera's method

In the verification of Patera's method, we compared POC obtained by Patera's method and the POC obtained by another model. The model we compared is SOCRATES, which is provided by Celestrak's homepage [2]. This model presents the analysis results over the next a week period and uses SGP4 analytical orbit model. And it conducts analysis when the relative distance reaches within 5 km and presents the result as maximum POC and miss distance which are the closest distance between two satellites.

Table 3. Comparison of result between SOCRATES and Patera

PCA		COSMOS 1408 DEB	LEMUR-2-NICHOL
Radial [km]	X	1119.8848	1119.8706
	Y	-876.3214	-876.3283
	Z	-6787.7794	-6787.8026
Velocity [km/s]	X	1.434318	-1.633534
	Y	-7.333349	7.258231
	Z	1.188911	-1.271271
Miss-distance		0.028 km	
TCA		2022. 12. 07. 10:11:48.377 UTC	
POC	SOCRATES	1.879×10^{-3}	
	Patera	1.696×10^{-3}	

Table 3 shows the results of analyzing the POC between one of the fragments of COSMOS 1408 and LEMUR-2-NICHOL analyzed by SOCRATES on December 6, 2022, and the results of analysis using Patera's method. It can be found that the results obtained by Patera's method and the results of SOCRATES were similar. It is regarded that the error generated here was caused by the difference between the calculation method and the covariance ellipsoid.

4. Case Study

4.1 Actual Case

We conducted a case study based on actual cases to confirm that our model works properly. The actual case analyzed in this study were the FY 1C destroyed by China's ASAT test on January 11, 2007, and the COSMOS 1408 satellite destroyed by the Russian ASAT system named 'Nudol' conducted on November 15, 2021.

The FY 1C satellite, which was destroyed on January 11, 2007, was a Chinese meteorological satellite orbiting in SSO at an altitude of about 850 km, creating more than 3,000 fragments after the ASAT test, causing a major threat to nearby satellites. Actually, in June 2007, five months after the ASAT test, the U.S. TERRA satellite did an evacuation maneuver to avoid fragments from FY 1C [4], and one of the fragments collided with Russia's BLITS satellite in 2013 [41]. Therefore, to demonstrate the situation at that time, the collision risk analysis was carried out for the NOAA 18 of the U.S. orbiting at a similar altitude, the TERRA of the U.S., and the Arirang-2 operating in Korea at the time.

Russia's COSMOS 1408 satellite, which was destroyed on November 15, 2021, was in orbit at an altitude of 450km, and its fragments generated by an ASAT test threatened the International Space Station (ISS) orbiting at an altitude of 420 km, and ISS crew evacuated from this threatening [41, 43]. In this study, the ISS was selected as an analysis object to demonstrate the situation at the time, and Arirang-3A and Arirang-5, which were operated in Korea at the time, were also selected as analysis objects to analyze the collision risk.

4.2 Hypothetical Case

The hypothetical case dealt with in this study assumed that KMS 4, operated by North Korea, was destroyed due to an ASAT test, explosions, or unintended collisions.

Prior to this assumption, North Korea conducted several intercontinental ballistic missile (ICBM) tests in 2022, and some opinions have appeared that such tests might be carried out to test their ability of the direct ascent anti-satellite missile targeting on KMS 4 [42]. Although it is not clear whether North Korea has the capability to possess ASAT, given that they have already launched KMS 4 into orbit in February 2016, and the maximum altitude of the ICBM launched on March 24, 2022, reached 6,200 km [42], it can be estimated that they have the technologies close to intercepting satellites operating below 2,000 km.

The ISS was selected as a target object for risk analysis of the fragmented KMS 4 because it is the largest and human-inhabited satellite among many satellites flying at similar altitudes. The ISS orbits the Earth with an inclination angle of 51.6° at an altitude of about 400 km, similar to that of KMS 4, and the encounter angle is about 135.4 degrees, which can cause disastrous damage to satellites in the event of a collision.

The last hypothetical case assumed that North Korea intentionally intercepts KMS 4 to damage the ISS indirectly. In order for North Korea to indirectly attack a satellite of other countries, they would first find the point at which the distance between KMS 4 and the target satellite is closest. And then they will break up the satellite right before that point arrives, maximizing the POC by generating the debris clouds.

4.3 Parameter of Case Study

From now on, we will refer to the two real cases mentioned above as case 1 and case 2, respectively, and to the two hypothetical cases as case 3 and case 4. The TLE for each case can be found on NORAD's Celestrak website [2].

For case 1 and case 2, the TLEs before FY 1C and COSMOS 1408 were destroyed, and the TLEs of satellites subject to risk analysis at the point closest to that time were obtained, and they are arranged in table 4 and table 5.

With the state vector calculated by KOE obtained by TLE, the position and velocity vector of the target satellite were propagated until the point of satellite breakup, and it is accomplished that equalizing the time of the object. In the first case of FY 1C, the time was equalized based on 21:44:56 UTC on January 11, 2007, when the ASAT test occurred, and in the case of COMSMOS 1408, the time was equalized based on 02:50:00 UTC on November 15, 2021. KOE and state vector obtained by propagating each time are shown in table 4, table 5, table 7, and table 8.

For case 3 and case 4, the time of ISS, which is the subject of risk analysis, was taken as the criteria, and the TLE of ISS was obtained at 08:09:28 UTC on September 17, 2022, and the TLE of KMS 4 was obtained near that time. After that, the time of KMS 4 was eqaulized based on the time of ISS. KOE and state vector of case 3 and case 4 obtained by propagation are shown in table 6 and table 9.

In table 7-9, a means semi-major axis, e means eccentricity, i means inclination, ν means true anomaly, ω means argument of perigee and Ω means right ascension of ascending node.

Table 4. TLE data of case 1

FENGYUN 1C
1 25730U 99025A 07011.90621003 .00000180 00000+0 12153-3 0 9322
2 25730 98.6464 1.7411 0013513 266.0357 94.0215 14.11820274395460
TERRA
1 25994U 99068A 07011.76271310 .00000114 00000+0 35362-4 0 1278
2 25994 98.2236 88.3107 0000732 95.9992 264.1287 14.57098930375925
ARIRANG-2 (KOMPSAT-2)
1 29268U 06031A 07011.75892358 .00000099 00000+0 29327-4 0 5533
2 29268 98.1260 273.1502 0018913 51.3858 308.9036 14.61531667 2445
NOAA 18
1 28654U 05018A 07011.61594517 .00000288 00000+0 18419-3 0 7953
2 28654 98.8143 315.6637 0014444 354.5392 5.5612 14.11027555 84775

Table 5. TLE data of case 2

COSMOS 1408
1 13552U 82092A 21319.03826954 .00002024 00000+0 69413-4 0 9994
2 13552 82.5637 123.6906 0018570 108.1104 252.2161 15.29390138143134
ISS (ZARYA)
1 25544U 98067A 21319.09416832 .00000887 00000+0 24604-4 0 9991
2 25544 51.6443 316.5365 0004639 198.4186 273.5656 15.48575887311987
KOMPSAT-3A
1 40536U 15014A 21318.73975917 .00000685 00000+0 43277-4 0 9997
2 40536 97.5490 258.6127 0003141 129.9370 320.1162 15.12334468366596
ARIRANG-5 (KOMPSAT-5)
1 39227U 13042A 21319.10924941 -.00000507 00000+0 -31907-4 0 9996
2 39227 97.6272 142.5046 0002081 77.6399 58.9078 15.04500403452057

Table 6 TLE data of case 3 & 4

ISS (ZARYA)
1 25544U 98067A 22260.33990839 .00027540 00000+0 48646-3 0 9994
2 25544 51.6440 240.0404 0002584 264.4442 241.0983 15.50138426359471
KMS 4
1 41332U 16009A 22259.66809443 .00021163 00000+0 43758-3 0 9991
2 41332 97.2364 334.6862 0015724 358.1629 1.9560 15.45697486369915

Table 7. Keplerian Orbital Element of case 1

KOE	FY 1C	TERRA	KOMPSAT-2	NOAA 18
a [km]	7231.284	7075.168	7053.792	7227.901
e	0.00135129	0.00089402	0.00086714	0.00055566
i [deg]	98.6464	98.2268	98.1332	98.8180
ν [deg]	94.1759	232.7676	313.9906	34.4583
ω [deg]	266.0357	160.5951	101.7939	1.2308
Ω [deg]	1.7411	88.4482	273.2908	315.9448

Table 8. Keplerian Orbital Element of Case 2

KOE	COSMOS 1408	ISS	KOMPSAT-3A	KOMPSAT-5
a [km]	6837.387	6799.459	6918.278	6939.930
e	0.00152080	0.00058772	0.00204378	0.00116254
i [deg]	82.5536	51.6457	97.5429	97.6223
ν [deg]	262.3080	108.2539	143.2646	13.2417
ω [deg]	177.4846	136.9706	76.7655	171.0424
Ω [deg]	123.6121	316.4553	258.8923	142.5073

Table 9. Keplerian Orbital Element of Case 3 & 4

KOE	ISS	KMS 4
a [km]	6794.456	6800.009
e	0.0002584	0.0016898
i [deg]	51.6440	97.2403
ν [deg]	241.0723	141.4439
ω [deg]	264.4442	359.7876
Ω [deg]	240.0404	335.3657

Table 10. Cartesian state vector of Case 1

Cartesian		FY 1C	TERRA	Arirang-2	NOAA 18
Radial [km]	X	7228.7160	716.9655	-595.8230	3767.7219
	Y	215.7153	5895.1604	-4004.8036	-4544.4878
	Z	26.4109	3852.9434	5770.8387	4164.9228
Velocity [km/s]	X	0.01650029	0.78396196	-0.95404347	-3.75693837
	Y	-1.11605674	-4.15273795	6.17801601	2.34759909
	Z	7.33928524	6.19816039	4.18314218	5.96424077
Epoch		2007. 01. 11. 21:44:56 UTC			

Table 11. Cartesian state vector of Case 2

Cartesian		COSMOS 1408	ISS	Arirang-3A	Arirang-5
Radial [km]	X	-1397.2866	-4705.3745	1596.3376	5442.9473
	Y	526.4144	-813.8999	5093.9181	-4261.9893
	Z	6673.7665	-4842.1755	-4418.4895	-513.2696
Velocity [km/s]	X	4.01524111	3.66366538	-0.18945184	-1.05896142
	Y	-6.35470397	-6.23173180	-4.92276348	-0.45253302
	Z	1.33012676	-2.51869732	-5.75827604	-7.49931347
Epoch		2021. 11. 15. 02:50:00 UTC			

Table 12. Cartesian state vector of Case 3 & 4

Cartesian		ISS	KMS 4
Radial [km]	X	4865.6330	-5049.6522
	Y	3660.5945	1724.4182
	Z	3016.9242	4229.6214
Velocity [km/s]	X	-1.22981771	-4.04485098
	Y	5.71189474	2.68067385
	Z	-4.95102271	-5.90898945
Epoch		2022. 09. 17. 08:09:28 UTC	

Since each case is either ASAT tests or hypothetical ASAT tests, missile data and colliding conditions are required to use the breakup model. In the case of the FY 1C ASAT test, the missile data are known through literature [4], but in the case of the Russian Nudol system that intercepted COSMOS 1408, the known missile data was used because it was difficult to know the information. In addition, in the case of hypothetical interception of KMS 4, other known missile data was used because it was expected to intercept similarly to ASAT tests of other countries. Table 13 shows the missile (Projectile) and target satellite (Target) data used in the case study.

Table 14 shows the parameter of the satellites obtained through various literature like websites, books, and paper, and the atmospheric drag coefficient () of all satellites and debris was assumed to be 2.0..

Table 13. Colliding condition of case study

	Projectile mass	Target mass	Collision Velocity
Case 1	18kg	950kg	8 km/s
Case 2	20kg	1750kg	8 km/s
Case 3	16kg	200kg	7 km/s

Table 14. Parameter of target satellite

	mass [kg]	A [m^2]	Size [m] (w, l, h)	L_c [m]
FY1C	950	3.3	1.5, 1.5, 1.5	2.6
TERRA	5190	23.8	3.5 3.5 6.	11.8
KOMPSAT-2	765	5.2	2, 2, 2.6	3.8
NOAA18	1479	8	1.9 1.9 4.2	5.0
COSMOS 1408	1750	4.16	1.0 1.3 3.2	3.6
ISS	419,725	931.57	73, 109, -	109
KOMPSAT3A	1,100	7.6	2, 2, 3.8	4.7
KOMPSAT-5	1,400	9.6	2.6, 2.6, 3.7	5.2
KMS 4	200	3.3	1.5 1.5 1.5	2.6

* Solar panel of each satellite is excluded

5. Result

In this chapter, the results of POC analysis for all cases mentioned in the previous chapter are presented. From case 1 to case 3, the closest distance between two objects (Miss-distance) and POC was analyzed by dividing the target satellite into whether it was broken or not over a period of 7 days, and they were compared with each other.

In case 4, as mentioned in the previous chapter, case of KMS 4 was not broken in case 3, the point when the minimum miss-distance is occur is used as the criteria time. And then we conducted the break-up of KMS 4 just before the criteria time comes.

5.1 FY 1C ASAT Test (Case 1)

In Case 1, the case of ASAT test in which FY 1C was broken was described. Table 15 shows the miss-distance and POC before and after breakup of FY 1C, and POC at the closest miss-distance is classified as (a) and miss-distance at the maximum POC appeasr during the entire period as (b). Fig. 10 - 12 show the changes in miss-distance and POC in case 1 without breakup and after breakup as graphs for time.

If FY 1C had not been broken, FY 1C satellite would not have been approached within 100km to the TERRA satellite, Arirang-2, and NOAA 18, and the POC would have been very low. In the contrast, after the FY 1C break-up, the number of cases in which fragments generated from FY 1C approached the within 100 km to those target satellites was increased. And, minimum miss-distance reach within 20.091 km, 30.925 km, and 7.032 km, respectively.

The maximum POC was $1.786\times10^{-5}(\%)$, $1.268\times10^{-6}(\%)$, and $4.245\times10^{-5}(\%)$, respectively, which increased significantly compared to those of before break-up.

Table 15. POC analysis result of case 1

Target Satellite			Time [min]	Miss-dist [km]	POC [%]
TERRA	Before	(a)	6190	170.0102	4.441e-19
		(b)	same as above		
	After	(a)	8017	20.091	1.127e-5
		(b)	2487	164.463	1.786e-5
Arirang-2	Before	(a)	2321	174.721	4.442e-19
		(b)	same as above		
	After	(a)	1090	30.925	6.954e-7
		(b)	3256	58.286	1.268e-6
NOAA 18	Before	(a)	10063	2660.616	0
		(b)	same as above		
	After	(a)	2870	7.032	3.769e-6
		(b)	3023	33.148	4.245e-6

(a): Result based on minimum miss-distance
(b): Result based on Maximum POC

According to the result, FY 1C fragments may not pose a significant threat to the target satellite. However, as can be seen in the results, the miss-distance was further closed, and the POC was also increased, indicating that the FY 1C breakup was of interest to satellite operators.

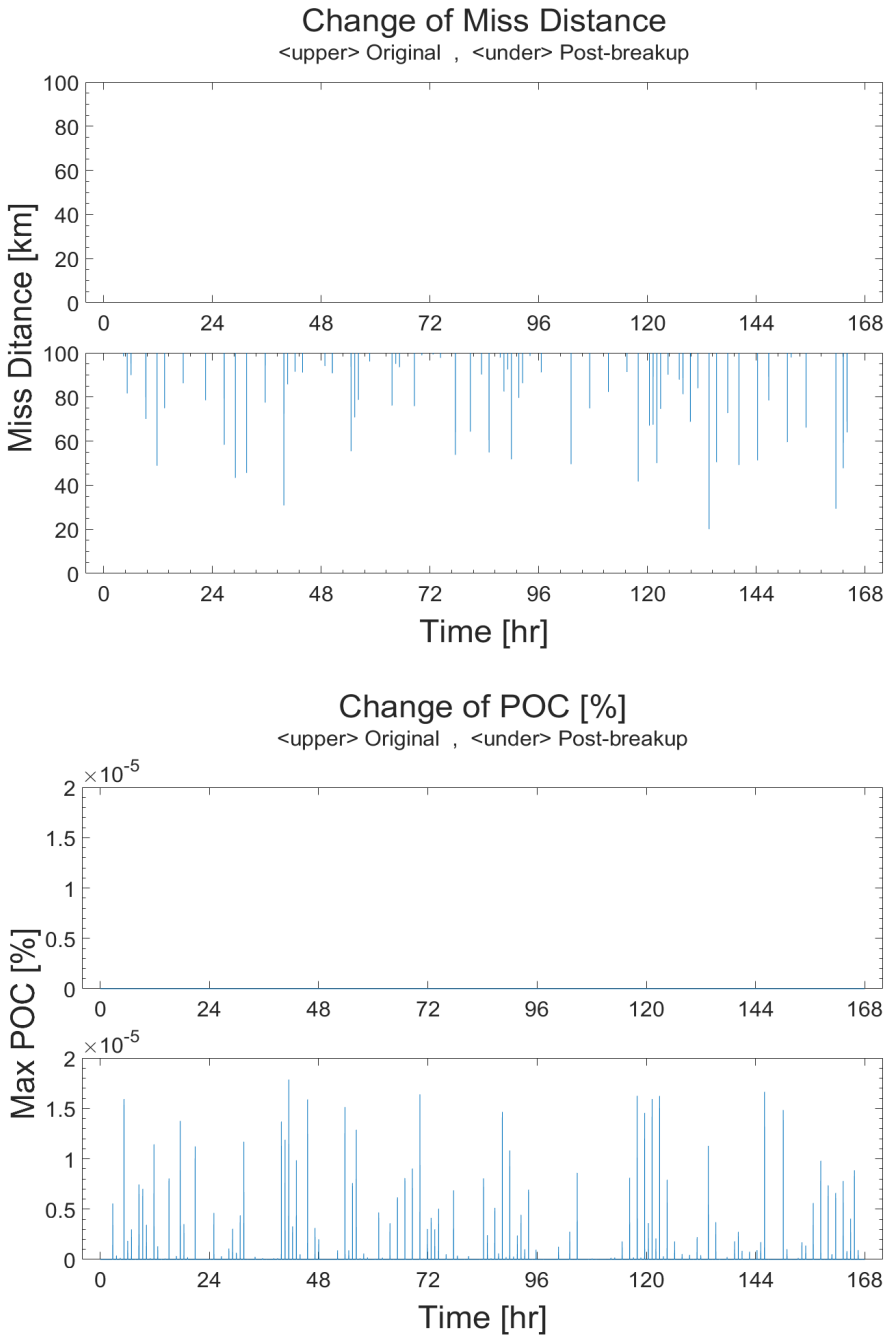

Fig. 10 Change of miss-distance and POC of case 1
< target: TERRA >

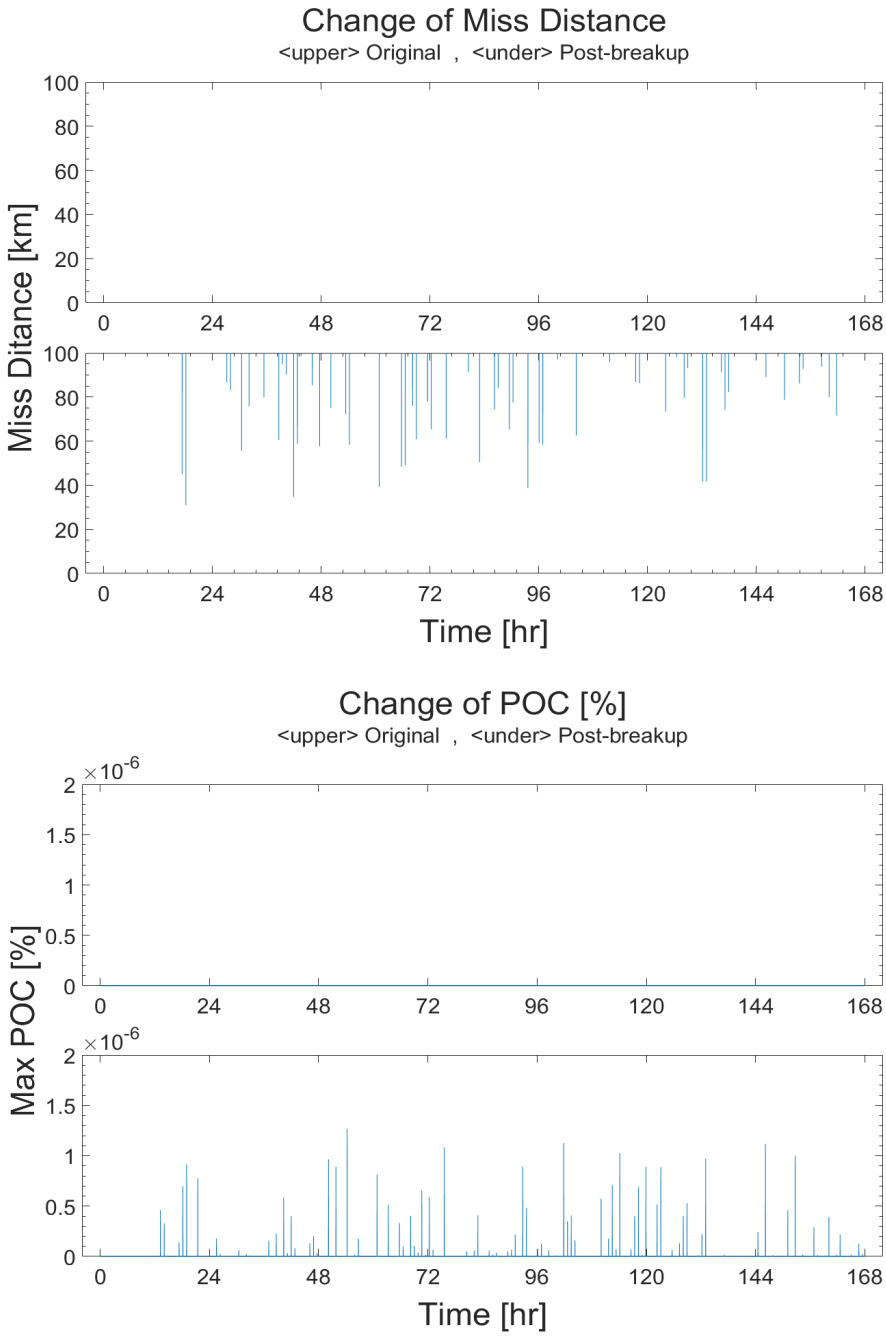

Fig. 11 Change of miss-distance and POC of Case 1

< target: Arirang-2 >

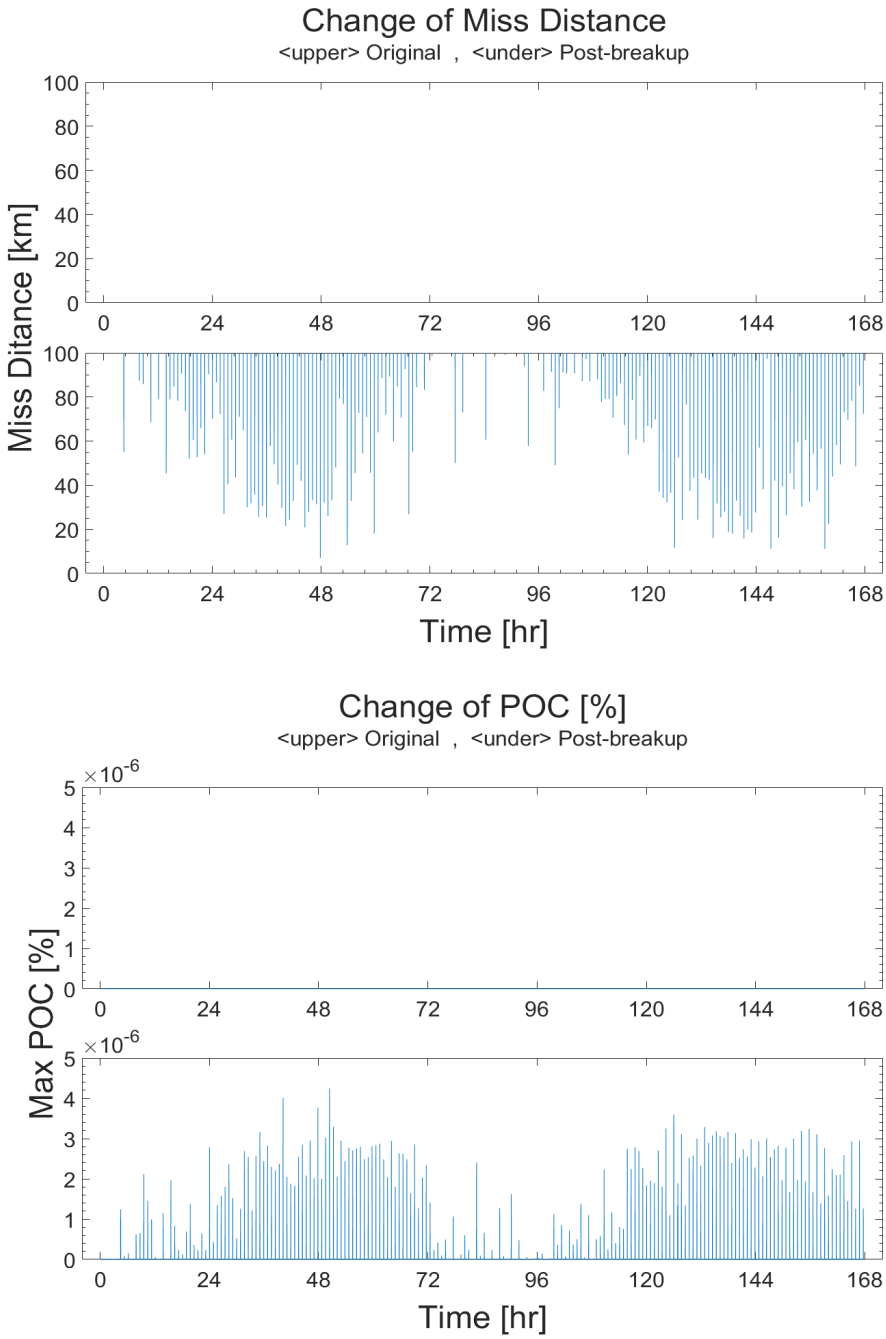

Fig. 12 Change of miss-distance and POC of case 1

< target: NOAA 18 >

5.2 COSMOS 1408 ASAT Test (Case 2)

In case 2, the case of the ASAT test was described for the COSMOS 1408 at 02:50 UTC on November 15, 2021. Table 16 shows the miss-distance and POC before and after break-up of COSMOS 1408, and POC at the closest miss-distance is classified as (a), and the miss-distance at the maximum POC appears during the entire period as (b). Fig. 13 - 15 show the changes in miss-distance and POC in case 2 without breakup and after breakup as graphs for time.

From these results, it can be seen that if COSMOS 1408 had not broken, the case in which the miss-distance is within 100 km would have not occurred for 7 days. except for only two times of ISS comes within 100 km. And we can see that POC for the target satellites is very low.

However, after COSMOS 1408 breakup, the number of cases in which fragments generated from COSMOS 1408 approached within 100 km to those target satellites increased. Notably, in the case of ISS in case 2, miss-distances approached to within 100 km appeared for the almost whole period, and minimum miss-distance appeared up to 3.851 km. And POC rose to $1.901\times10^{-3}(\%)$ for ISS, $9.628\times10^{-6}(\%)$ for Arirang-3A, and $6.994\times10^{-6}(\%)$ for Arirang-5. Especially, the POC of ISS was higher than $1.0\times10^{-3}(\%)$ for almost the period, which means it could pose a significant threat to the ISS.

From these result, Not only did it prove well that ASAT test for COSMOS 1408 posed a threat to the ISS, but it could also be inferred that it became of interest to Korean satellite operators.

Table 16. POC analysis result of case 2

Target Satellite			Time [min]	Miss-dist [km]	POC [%]
ISS	Before	(a)	9102	60.08	4.4034e-5
		(b)	9101.67	294.5417	7.3168e-6
	After	(a)	5657.5	3.8514	1.4851e-3
		(b)	5750.5	52.3571	1.9016e-3
Arirang-3A	Before	(a)	2306	242.77	8.3452e-38
		(b)	same as above		
	After	(a)	4168.33	22.9905	5.5177e-6
		(b)	4120.83	99.2495	9.6289e-6
Arirang-5	Before	(a)	1500	299.8234	3.7976e-8
		(b)	same as above		
	After	(a)	5285.17	43.2372	2.317e-6
		(b)	2026.83	204.7844	6.9948e-6

(a): Result based on minimum miss-distance

(b): Result based on Maximum POC

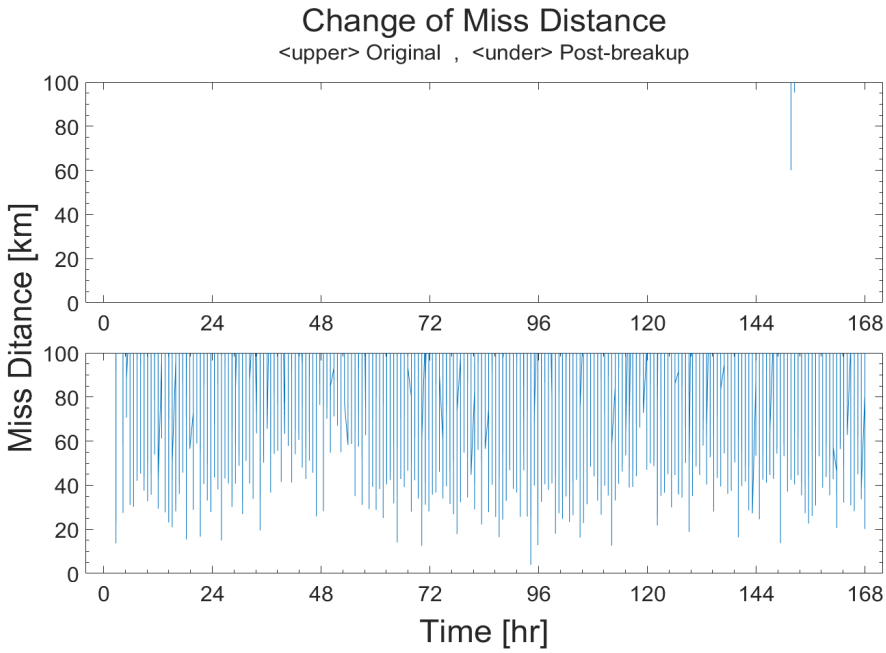

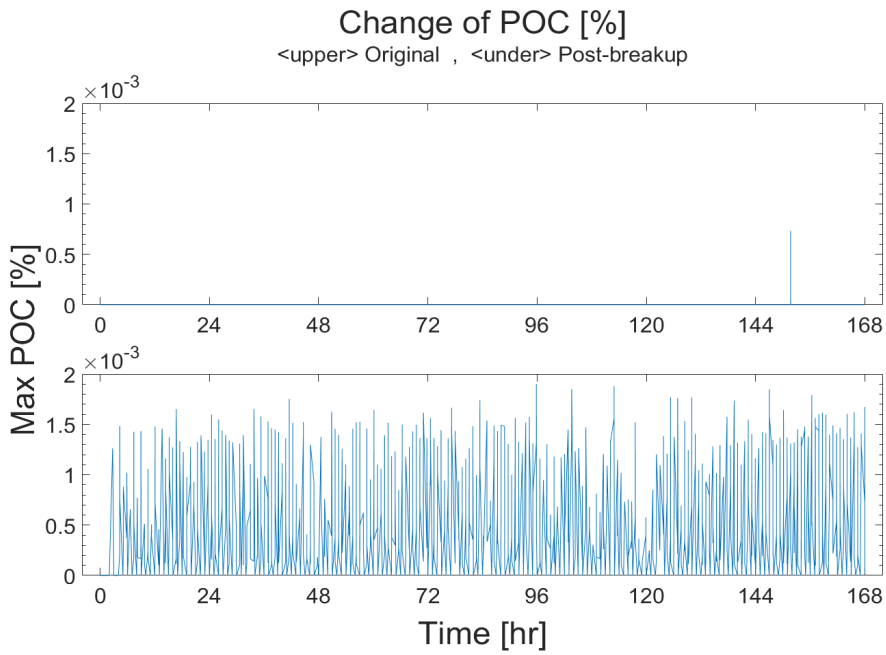

Fig. 13 Change of miss-distance and POC of case 2

< target: ISS >

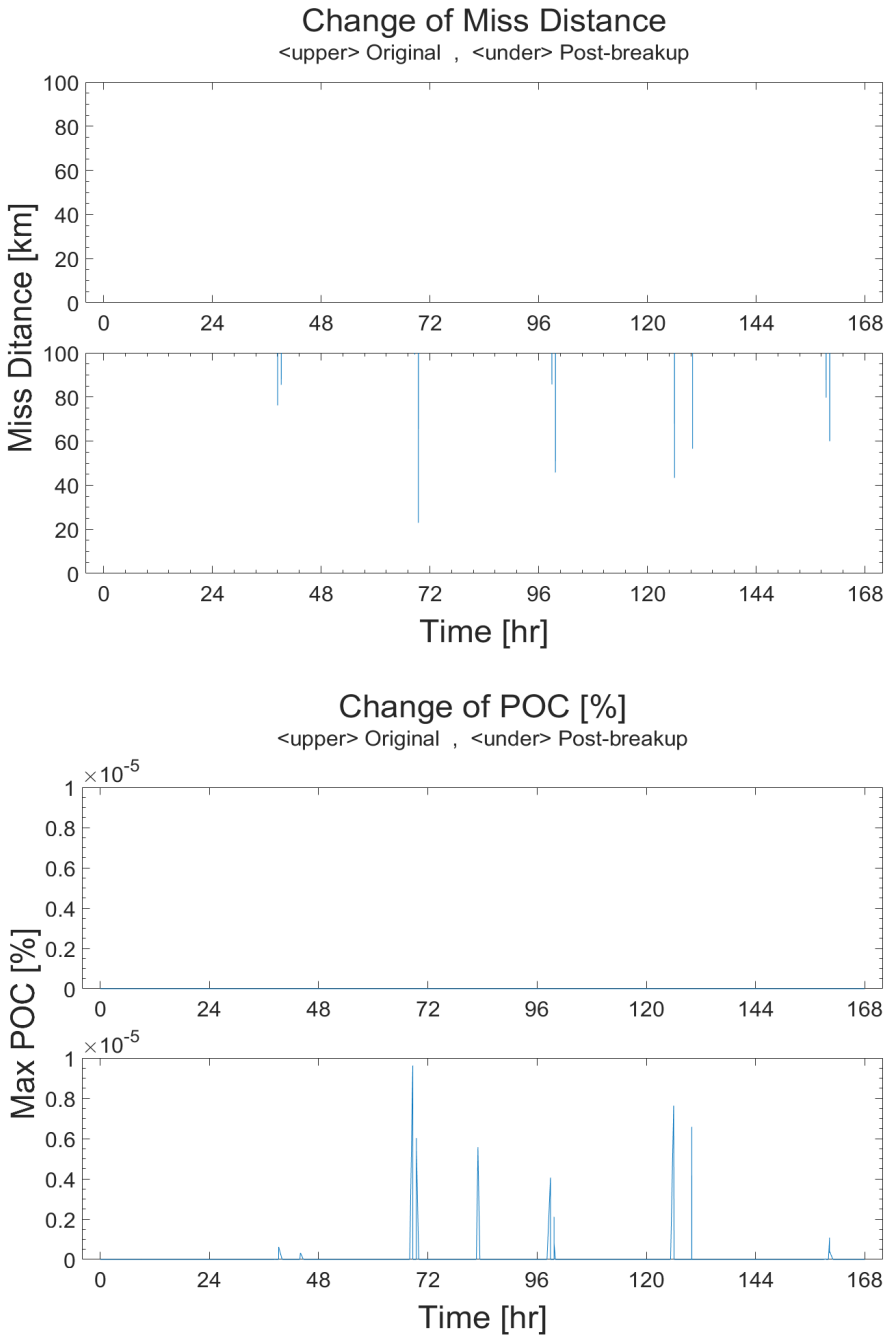

Fig. 14 Change of miss-distance and POC of case 2

< target: Arirang-3A >

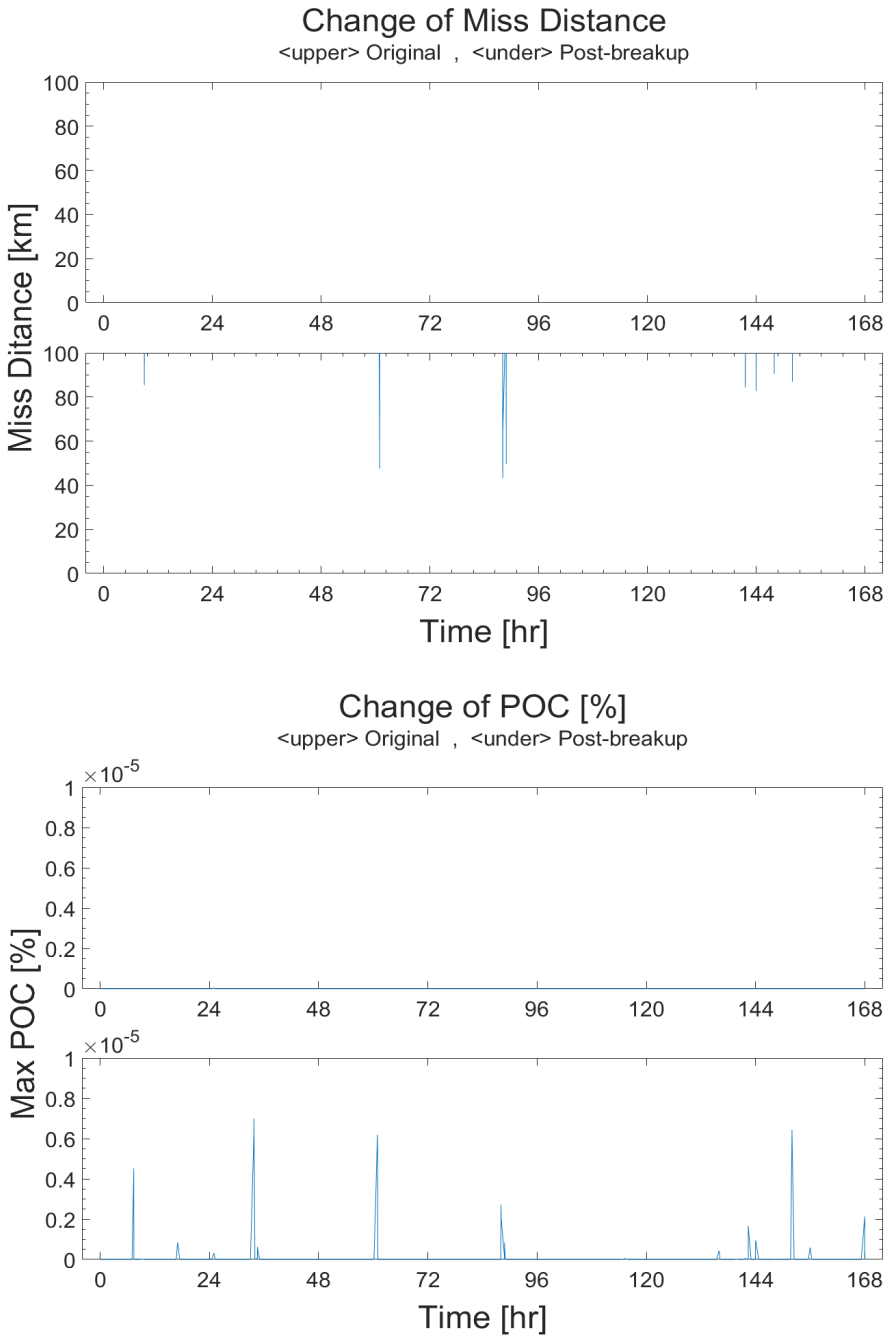

Fig. 15 Change of miss-distance and POC of Case 2

< target: Arirang-5 >

5.3 KMS 4 Break-up by Hypothetical ASAT Test (Case 3)

In case 3, it was assumed that North Korea conducted the ASAT test on their satellite, KMS 4. As a target satellite, ISS orbiting at a similar altitude was selected. The analysis period was selected arbitrarily for 7 days from 08:09:28 UTC on September 17, 2002.

Table 17 shows the results of the analysis of miss-distance and POC for 7 days from the reference time. As in the previous section, it was classified into the case of (a) and (b).

As a result, cases of approaching KMS 4 and ISS within 100 km appeared between about after 48 hours and after 53 hours, approaching miss-distance as 33.024 km after 3048 minutes and 40 seconds, and the POC at this time was $5.328 \times 10^{-4}(\%)$. The maximum POC appeared after 3095 minutes and 20 seconds and it was $7.514 \times 10^{-4}(\%)$.

On the other hand, in the analysis between the fragments generated after the breakup of KMS 4 and the ISS, they are approached within 100 km for almost of the period, and they approached up to 3.853 km after 3048.67 minutes from the breakup. At this time, POC was analyzed as $1.604 \times 10^{-4}(\%)$, and the maximum POC over the all period was anlyzed as $1.627 \times 10^{-3}(\%)$. The POC shown in this result can have a significant adverse effect on satellite operators. This means that if KMS 4 breaks up, it could be a severe threat to the ISS.

Table 17. POC analysis result of case 3

Target Satellite			Time [min]	Miss-dist [km]	POC [%]
ISS	Before	(a)	3048.67	33.024	5.328e-4
		(b)	3095.33	110.760	7.514e-4
	After	(a)	3048.67	3.853	1.604e-3
		(b)	2863.00	11.678	1.627e-3

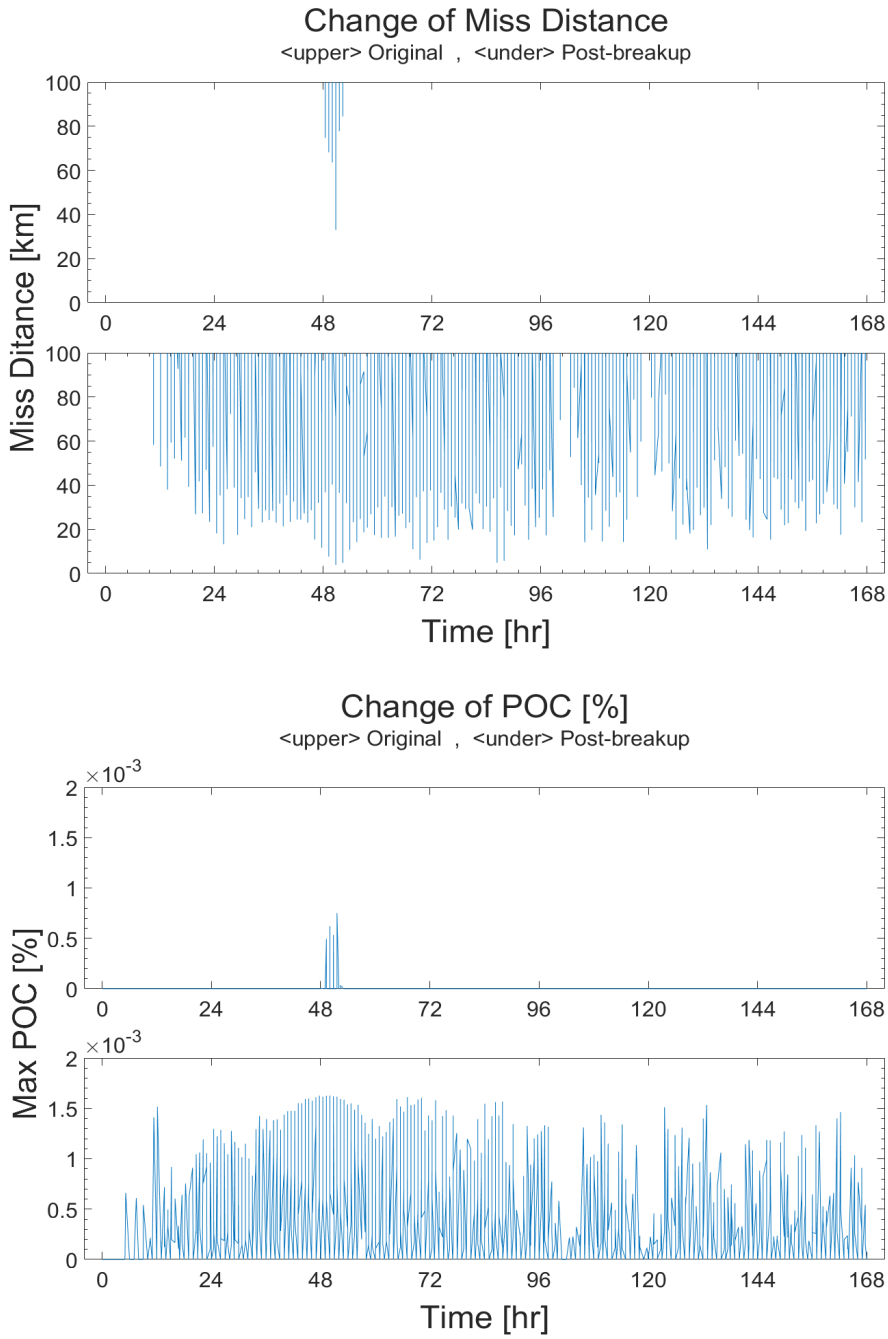

Fig. 16 Change of miss-distance and POC of Case 3

< broken: KMS 4 , target: ISS >

5.4 KMS 4 break-up right before reaching the highest probability

In the analysis of Case 4, it was assumed that North Korea intentionally attacked the ISS. In order to cause damage to the ISS definitely, the time when the distance between KMS 4 and ISS becomes closest could be determined as the optimal time. Therefore, in order to increase the POC as much as possible, it is necessary to increase the POC by generating debris clouds by breaking up KMS 4 earlier than that time.

Under this assumption, the minimum miss-distance after 3048.67 minutes was adopted as the criteria time, when KMS 4 was not broken in Case 3. And we conduct some simulations that KMS 4 was broken every 1 minute from the criteria time to 10 minutes before, and every 10 minutes from the criteria time to 100 minutes before.

The miss-distance and POC at the reference point after the break-up were analyzed, and the minimum miss-distance within 4 hours after the break-up and the POC at that time are shown in Table 18. In addition, Fig. 17 - 20 show the changes in miss-distance and POC within 4 hours from criteria time as graphs for time.

As a result of the analysis, it was found that when KMS 4 was broken from 3 to 5 minutes before reaching the minimum miss-distance, the closest miss-distance appeared, and the POC also increased significantly. And, when KMS 4 broke up 20-100 minutes before the criteria time, almost all of the minimum miss-distances appeared, and most of the POC was reached over $1.6 \times 10^{-3}(\%)$. Analysis within 4 hours shows that the minimum miss-distance mainly appeared after 92.67 minutes, which is the period of KMS 4

orbiting once, and the POC was also reached over 1.4×10^{-3}(%).

From these results, it was found that in order to attack other satellites by debris clouds, the effective attack was possible when the break-up of a satellite occurred at least from 3 to 5 minute before reaching the minimums distance. Furthermore, in case of the break-up of satellite right before the minimum miss-distance between the two satellites appears, the optimal range of break-up can be inferred between 5 minutes to 1 period before, based on the result that the POC after 1 period is appeared generally high.

Table 18. POC analysis result of case 4

Break-up Time before criteria	At criteria time		Within 4 Hours		
	Miss-dist [km]	POC [%]	Time [min]	Miss-dist [km]	POC [%]
0	33.024	5.328e-4	92.67	5.193	1.542e-3
1 min	26.754	6.739e-4	92.67	6.235	1.525e-3
2 min	28.462	6.528e-4	92.67	6.391	1.562e-3
3 min	12.171	1.370e-3	185.50	8.664	1.536e-3
4 min	21.615	1.108e-3	92.67	4.077	1.549e-3
5 min	11.850	1.552e-3	92.67	4.975	1.554e-3
6 min	17.310	1.606e-3	185.50	4.416	1.547e-3
7 min	12.518	1.385e-3	92.67	1.501	1.582e-3
8 min	20.547	1.230e-3	92.67	7.362	1.508e-3
9 min	16.783	1.576e-3	185.50	8.959	1.555e-3
10 min	13.588	1.571e-3	92.67	3.919	1.575e-3
20 min	3.673	1.601e-3	92.67	11.221	1.406e-3
30 min	2.165	1.604e-3	92.67	8.029	1.549e-3
40 min	4.116	1.564e-3	92.67	19.538	1.406e-3
50 min	2.701	1.575e-3	92.67	9.944	1.489e-3
60 min	1.829	1.619e-3	92.67	9.663	1.523e-3
70 min	0.689	1.618e-3	92.67	6.114	1.580e-3
80 min	1.994	1.628e-3	185.50	4.150	1.569e-3
90 min	4.045	1.619e-3	92.67	6.425	1.546e-3
100 min	2.532	1.604e-3	92.67	3.821	1.544e-3

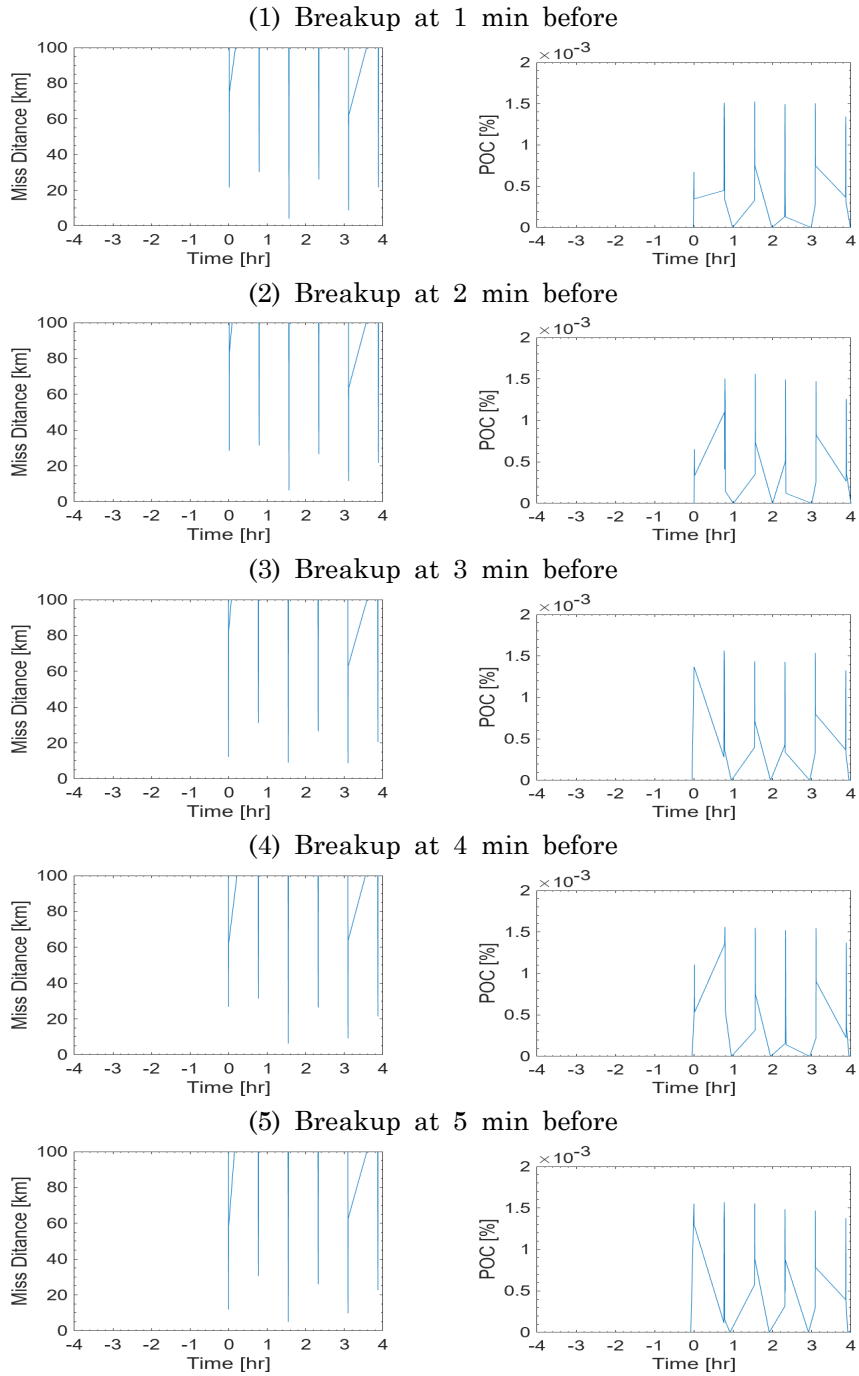

Fig. 17 Miss-distance (left) & POC (right) analysis of case 4

(6) Breakup at 6 min before

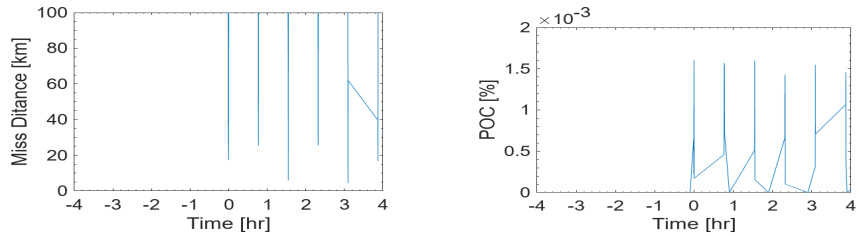

(7) Breakup at 7 min before

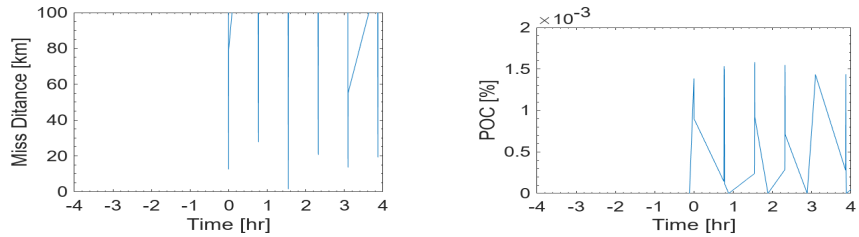

(8) Breakup at 8 min before

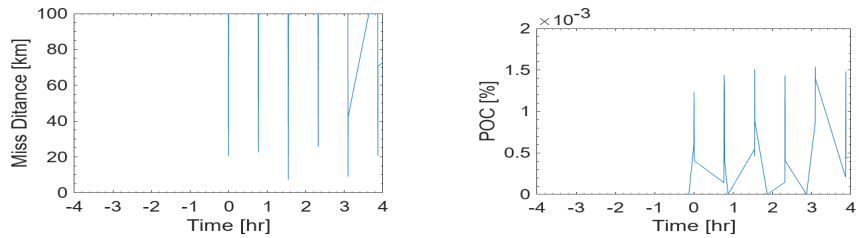

(9) Breakup at 9 min before

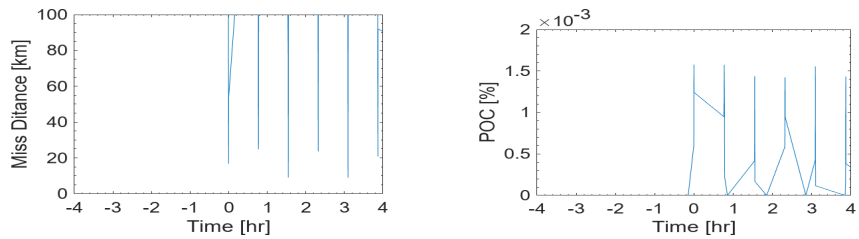

(10) Breakup at 10 min before

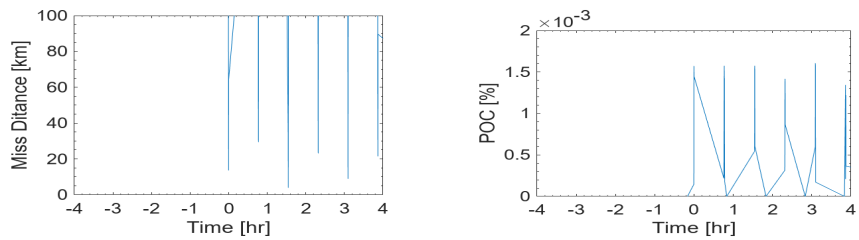

Fig. 17 Miss-distance (left) & POC (right) analysis of case 4

(11) Breakup at 10 min before

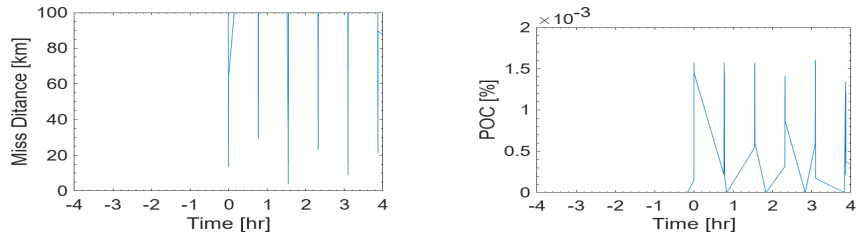

(12) Breakup at 20 min before

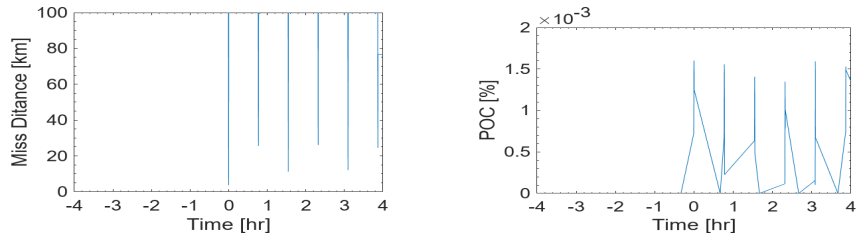

(13) Breakup at 30 min before

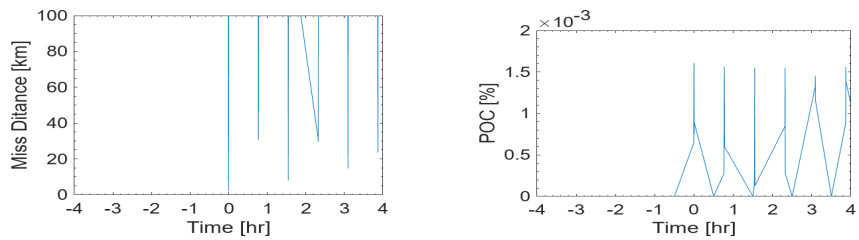

(14) Breakup at 40 min before

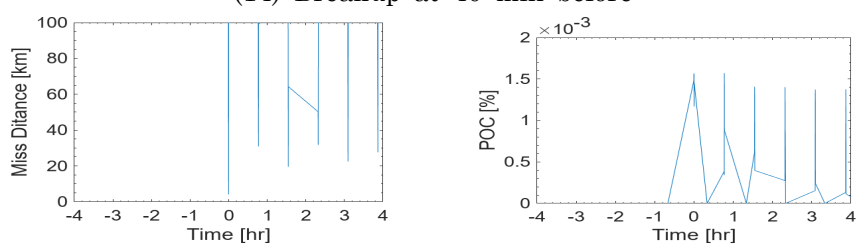

(15) Breakup at 50 min before

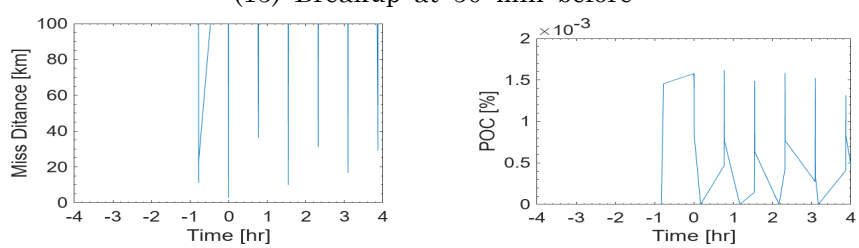

Fig. 17 Miss-distance (left) & POC (right) analysis of case 4

(16) Breakup at 60 min before

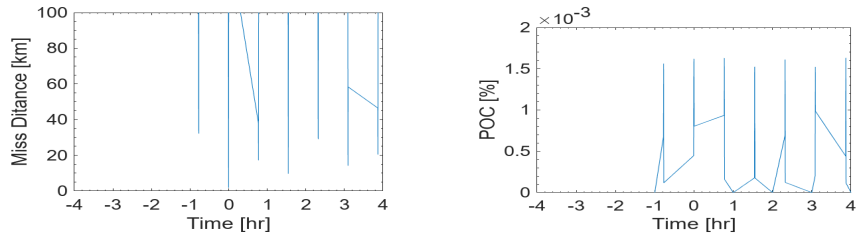

(17) Breakup at 70 min before

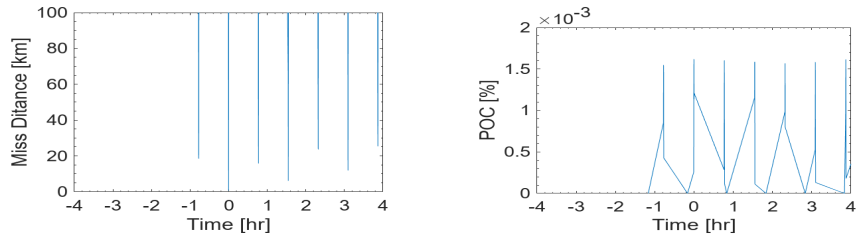

(18) Breakup at 80 min before

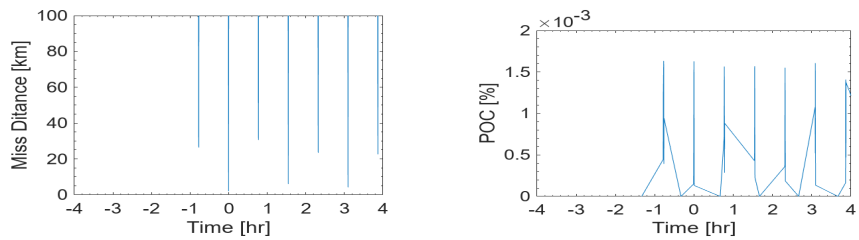

(19) Breakup at 90 min before

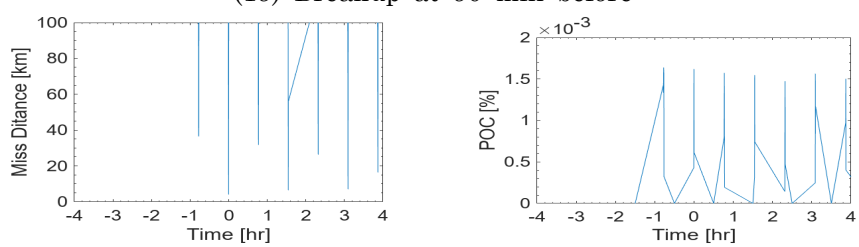

(20) Breakup at 100 min before

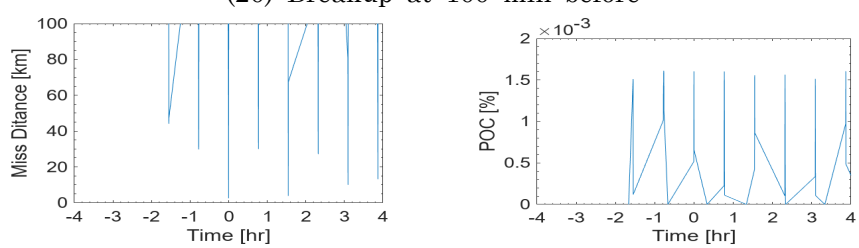

Fig. 17 Miss-distance (left) & POC (right) analysis of case 4

6. Discussion

The case study of the break-up of Cosmos 1408 in case 2 showed similar results to the actual case that posed a significant threat to the ISS. In this case study, it was confirmed that not only the miss-distance became quite close during the 7-day analysis period, but also the POC increased to a level to be careful, posing a great threat to the ISS crew at that time. Through our study, it can be seen that this study can show results that can sufficiently analyze the risk even if it is not completely the same as the actual event.

Another notable result in the case study was that the POC does not always increase to the maximum, even two satellites are orbiting at similar altitudes. In the case study between FY 1C fragments and TERRA and NOAA 18, the miss-distance was closer to the TERRA satellite, which was about 150 km apart than the NOAA 18 satellite at a similar altitude, and the POC was higher in the case of the TERRA.

This means that even if the satellites break up, they may not immediately pose a threat to satellites on similar altitudes. In fact, at that time, FY 1C and NOAA 18 were orbiting in SSO, in which the inclination is 98 degrees, but there were differences in orbital planes, and these two satellites did not encounter each other closely due to differences in their positions in orbit. Therefore, even if the two satellites are at similar altitudes, they may not be threatening each other if they do not encounter each other closely, and it can be seen that the analysis should be performed except in this case.

The case study in case 3 shows that if North Korea conducts an ASAT test, it could pose a great threat to the operation of

satellites in other countries. Especially, case 4 showed that if North Korea intentionally tries to attack another satellite, the most threatening attack could be made if the test was conducted about 5 minutes to 1 period before at the time of minimum miss-distance between KMS 4 and Target. So, our study can help satellite operators determine whether evacuation maneuvers of satellites should be performed in situations where the ASAT test may occur.

7. Conclusion

Through the present study, the risk of fragments generated after the break-up of a space object on other satellites was analyzed. So that, NASA's Evolve 4.0 Breakup model among the existing satellite breakup models and Patera's method among the analyzing POC method were combined. After that, case studies were conducted through actual break-up cases and hypothetical break-up cases. Through these case studies, it was possible to reproduce the environment caused by fragments generated from the break-up of a space object, and it was possible to analyze the risk of collision with a satellite.

From the present study, it was found that the risk of collision could be maximized if a space object breaks up right before the minimum miss-distance of the two space objects is reached. And notably, it was found that the threat of fragments generated from the break-up of a space object to other satellites could vary depending on the conditions of the KOE of the satellite.

Therefore, satellite operators need to continuously track satellites that may pose a threat to satellite operation, and this method will

be able to identify risks in a short period in the event of a satellite break-up situation. This will greatly help the operation of the satellite.

Furthermore, if the R.O.K. Armed Forces utilize this study, it can be used as a basic study that can have a positive impact on space security as well as improve its ability to respond to threats in the space domain. In addition, by developing this study, it will be possible to use it as an indirect satellite interception system that can indirectly intercept satellites hostile to space security. This will be an important factor in taking the initiative in possible future space wars.

In order to prepare for these, we plan to make up for some of the deficiencies in our study. First, we will study how to predict the fragment's orbit more accurately. Second, we will accumulate big data through various case studies. Lastly, we will study the degree of damage to the satellite when fragments collide with the satellites. If these are supplemented, it is expected to contribute greatly to space security.

Bibliography

[1] Ben-Larbi, Mohamed Khalil, et al. "Towards the automated operations of large distributed satellite systems. Part 1: Review and paradigm shifts." Advances in Space Research 67.11 (2021): 3598-3619.

[2] "Celestrak". *Celestrak,* https://celestrak.org/.

[3] ESA Space Debris Office. ESA's Annual Space Enviroment Report. Germany, ESA Space Debris Office, 2022.

[4] Tan, Arjun, and Robert C. Reynolds. Theory of satellite fragmentation in orbit. World Scientific, 2019.

[5] Kessler, Donald J., and Burton G. Cour Palais. "Collision frequency of artificial satellites: The creation of a debris belt." Journal of Geophysical Research: Space Physics 83.A6 (1978): 2637-2646.

[6] Johnson, Nicholas L., et al. History of on-orbit satellite fragmentations. No. S-1030. 2008.

[7] Wang, Ting. "Analysis of Debris from the Collision of the Cosmos 2251 and the Iridium 33 Satellites." Science & Global Security 18.2 (2010): 87-118.

[8] Liou, J. C., and D. Shoots. "Satellite collision leaves significant debris clouds." Orbital Debris Quarterly News

13.2 (2009): 1.

[9] Sorge, Marlon. "Satellite fragmentation modeling with IMPACT." AIAA/AAS Astrodynamics Specialist Conference and Exhibit. 2008.

[10] Sorge, Marlon, and Deanna Mains. "Impact fragmenation model improvements." AIAA/AAS Astrodynamics Specialist Conference. 2014.

[11] Frey, Stefan, and Camilla Colombo. "Transformation of satellite breakup distribution for probabilistic orbital collision hazard analysis." Journal of Guidance, Control, and Dynamics 44.1 (2021): 88-105.

[12] Andrişan, Roxana Larisa, et al. "Fragmentation event model and assessment tool (FREMAT) supporting on-orbit fragmentation analysis." 7th European Conference on Space Debris. 2017.

[13] Johnson, Nicholas L., et al. "NASA's new breakup model of EVOLVE 4.0." Advances in Space Research 28.9 (2001): 1377-1384.

[14] Joubert, Wynand, and Steven Tingay. "Simulations of orbital debris clouds due to breakup events and their characterisation using the Murchison Widefield Array radio telescope." Experimental Astronomy 51 (2021): 61-75.

[15] Choi, Su-Jin, In-Sik Jung, and Dae-Won Chung. "Current Status of Space Debris and Introduction of the KARI Conjunction Assessment Process." Current Industrial and Technological Trends in Aerospace 9.1 (2011): 55-63.

[16] Foster, James Lee, and Herbert S. Estes. A parametric analysis of orbital debris collision probability and maneuver rate for space vehicles. NASA, National Aeronautics and Space Administration, Lyndon B. Johnson Space Center, 1992.

[17] Chan, Ken. "Collision probability analysis for earth orbiting satellites." Space cooperation into the 21 st century (1997): 1033-1048.

[18] Chan, Ken. "Improved analytical expressions for computing spacecraft collision probabilities." Advances in the Astronautical Sciences 114 (2003): 1197-1216.

[19] Chan, Ken. "Spacecraft collision probability for long-term encounters." Advances in the Astronautical Sciences 116.1 (2003): 767-784.

[20] Chan, Ken. "Short-term vs. long-term spacecraft encounters." AIAA/AAS astrodynamics specialist conference and exhibit. 2004.

[21] Patera, Russell P. "General method for calculating satellite

collision probability." Journal of Guidance, Control, and Dynamics 24.4 (2001): 716-722.

[22] Patera, Russell P. "Method for calculating collision probability between a satellite and a space tether." Journal of Guidance, Control, and Dynamics 25.5 (2002): 940-945.

[23] Patera, Russell P. "Calculating collision probability for arbitrary space vehicle shapes via numerical quadrature." Journal of guidance, control, and dynamics 28.6 (2005): 1326-1328.

[24] Patera, Russell P. "Application of symmetrized covariances in space confliction prediction." Advances In Space Research 34.5 (2004): 1115-1119.

[25] Patera, Russell P. "Conventional form of the collision probability integral for arbitrary space vehicle shape." AIAA/AAS Astrodynamics Specialist Conference and Exhibit. 2004.

[26]. Alfano, Salvatore. "A numerical implementation of spherical object collision probability." The Journal of the Astronautical Sciences 53 (2005): 103-109.

[27] Alfano, Salvatore. "Addressing nonlinear relative motion for spacecraft collision probability." AIAA/AAS astrodynamics specialist conference and exhibit. 2006.

[28] Alfano, Salvatore, and Daniel Oltrogge. "Probability of Collision: Valuation, variability, visualization, and validity." Acta Astronautica 148 (2018): 301-316.

[29] Bérend, Nicolas. "Estimation of the probability of collision between two catalogued orbiting objects." Advances in Space Research 23.1 (1999): 243-247.

[30] Alfriend, Kyle T., et al. "Probability of collision error analysis." Space Debris 1.1 (1999): 21-35.

[31] Akella, Maruthi R., and Kyle T. Alfriend. "Probability of collision between space objects." Journal of Guidance, Control, and Dynamics 23.5 (2000): 769-772.

[32] Vedder, John D., and Jill L. Tabor. "New method for estimating low-earth-orbit collision probabilities." Journal of Spacecraft and Rockets 28.2 (1991): 210-215.

[33] Serra, Romain, et al. "A new method to compute the probability of collision for short-term space encounters." AIAA/AAS Astrodynamics Specialist Conference. 2014.

[34] Vallado, David A. Fundamentals of astrodynamics and applications. Vol. 12. Springer Science & Business Media, 2001.

[35] Ruiter, Anton H. J. de, et al. Spacecraft Dynamics and Control: An Introduction. John Wiley & Sons, Ltd., 2013.

[36] Chen, Lei, et al. Orbital Data Applications for Space Objects. Springer, Singapore, Singapore,, 2017.

[37] Larson, Wiley J., and James Richard Wertz, eds. Space mission analysis and design. Vol. 3. Torrance, CA: Microcosm, 1992.

[38] Flohrer, Tim, Holger Krag, and Heiner Klinkrad. "Assessment and categorization of TLE orbit errors for the US SSN catalogue." risk 8.9 (2008): 10-11.

[39] Flohrer, Tim, et al. "Improving ESA's collision risk estimates by an assessment of the TLE orbit errors of the US SSN catalogue." Proc. of the 5th Europ. Conf. on Space Debris, Darmstadt, Germany ESA SP-672. 2009.

[40] Johnson, Megan R. NASA Robotic CARA Probability of Collision. No. GSFC-E-DAA-TN66334. 2018.

[41] Harrison, Todd, et al. Space threat assessment 2022. Center for Strategic & International Studies., 2022.

[42] Park, Daekwang. "North Korea's New Strategic Provocation Option, Possibility of Direct-Ascent Anti-Satellite Missile Test." Northeast Asia Strategic Analysis, Oct. 2022.

[43] Cowardin, Heather. "Orbital Debris Quarterly News." Orbital Debris Quarterly News 26.4 (2022).

초 록

최근 뉴스페이스 시대가 도래하면서 우주개발의 주체가 점차 민간으로 옮겨가고 있다. 이에 따라 인공위성은 소형화되고 있으며, 군집위성의 운영이 점점 증가하고 있다. 대조적으로 우주 공간에 대한 세계 각국의 관심이 높아져 가는 상황 속에서 일부 강대국들의 우주 패권경쟁을 위한 ASAT 무기를 개발 및 시험이 이루어지고 있다. 이로 인하여 우주에서의 인공물체들이 빠른 속도로 증가하고 있으며, 우주물체 간 상호 충돌 가능성 또한 급격하게 증가하고 있다. 만일 우주물체가 상호 충돌한다면 수 많은 파편들이 생겨나며 이 파편들이 다시 또 다른 인공위성들에게 충돌 위협을 가할 수 있다.

이러한 위험을 예측하기 위하여 본 연구에서는 우주물체가 분열한 이후 발생한 파편들이 인공위성에게 미치는 충돌위험을 분석하였다. 이를 위해 3단계의 과정을 통해 충돌위험을 분석하는 모델을 제시하였다. 첫 단계에서는 NASA EVOLVE 4.0 breakup model을 활용하여 우주물체의 분열로 인해 발생한 파편들을 묘사했으며, 두번째 단계에서는 수치적 궤도 모델을 활용하여 발생한 각각의 파편들의 궤도를 전파하였고, 마지막 단계에서는 Patera가 제시한 충돌확률 분석 방법을 활용하여 위험성을 분석하였다.

본 연구의 모델이 잘 작동하는지 검증하기 위하여 2007년 중국의 FY 1C 위성에 대한 ASAT 시험과 2021년 러시아의 COSMOS 1408 위성에 대한 ASAT 시험으로 사례 연구를 진행하였다. 또한 KMS 4 위성의 가상분열 시 ISS 위성에 대한 위험성 분석을 통해 가상의 사례 연구를

수행하였으며, ISS 위성에 근접하기 직전에 KMS 4 위성을 의도적으로 분열시키는 사례 연구를 통해 최대 충돌확률 발생 시점에 대한 분석을 수행하였다.

연구 결과 이 연구의 모델은 분열된 우주물체의 파편들의 특성을 실제 환경과 유사하게 묘사할 수 있었다. 또한 분열 이후 발생한 우주물체의 파편들에 의한 간접적인 위성 공격의 적절한 시점을 확인할 수 있었다.

본 연구를 활용하면 인공위성 운영자들에게 우주물체가 분열할 때를 대비할 수 있는 능력을 제공해 줄 수 있다. 또한 대한민국 국군도 이를 잘 활용하면 우주영역인식 능력을 향상할 수 있을 뿐만 아니라, 미래의 새로운 전장이 될지 모르는 우주 공간에서의 작전 능력을 향상할 수 있을 것으로 기대한다.

주요어 : NASA EVOLVE 4.0 위성분열모델, Patera 방법, 우주 파편, 인공위성, 최근접거리, 충돌확률
학 번 : 2021 - 28391

감사의 글

대한민국 육군 위탁교육생 신분으로 서울대학교 협동과정 우주시스템전공에 입학한 지 어느덧 2년이라는 시간이 흘러, 벌써 졸업을 앞두게 되었습니다. 육군의 우주력 발전에 크나큰 기여를 하겠다는 일념 하나로 지난 2년간 열심히 달려왔으나, 아직도 부족한 부분과 연구하고 싶은 것들이 너무나 많다는 것이 참 아쉬우면서도 이제는 지금까지 배우고 연구한 것들을 바탕으로 육군의 우주력 발전을 이루어내야 할 때라 생각하니 벌써부터 가슴 한켠이 벅차오르는 것 같습니다.

위탁교육을 받던 지난 2년을 돌아보니 제 주변엔 항상 감사한 분들이 계셨습니다. 우선 저에게 2년이라는 시간 동안 우주 분야에 대하여 연구할 수 있게 허락해주고 교육비 지원을 통해 별 다른 걱정 없이 연구에만 몰두할 수 있게 해준 대한민국 육군에게 먼저 감사의 인사를 올립니다.

다음으로 지난 2년간 저를 열심히 지도해주시고 항상 관심 가져 주시며 저를 많이 아껴주시던 저의 지도교수님이신 이복직 교수님께 정말 감사드립니다. 학부과정을 군사사학을 전공했던지라 공학 분야에 대한 지식이 전무함에도 불구하고 제가 잘 적응할 수 있도록 최선을 다해 지도해주심은 물론 다양한 학술적 경험을 할 수 있도록 도와주시고, 다양한 것들을 직접 보고 들을 수 있도록 지원을 아끼시지 않으셨던 교수님께 정말 감사드립니다. 저에게는 교수님의 지도와 관심이 지난 2년간의 대학원 생활의 큰 버팀목이자 원동력이 되었습니다.

그리고 비록 많이 미흡했지만 본 학위논문 심사에서 친절하게 임해주시고, 또 아낌없이 많은 조언을 해주셨던 김규홍 교수님과, 김현진 교수님께 감사의 인사 드립니다.

그리고 2021년도 1월 저의 첫 출근부터 약 1년간을 같은 연구실에서 함께 연구를 했던 권기범 교수님께도 감사의 인사 드립니다. 때로는 교수님의 위치에서 많은 지도를 해주셨고, 때로는 군 선배로써 군 생활에 도움이 될 수 있는 조언을 아끼시지 않으셨으며, 때로는 인생 선배로써 학생인 저를 아껴주시고 챙겨주셨기에 제가 대학원 생활을 빠르게 적응 할 수 있었습니다.

또한 지난 2년간 같은 연구실에서 함께 연구를 하였던 우리 항공우주추진 연구실 구성원들에게 정말 감사드립니다. 연구실의 대들보였던 이종권 형을 필두로 박윤식, 한서음, 전대영, 김주훈, 이정용, 김용수, 전병주, 홍슬기, 이종윤, 박정재, 송찬주, Rawdha Alhammadi, Karl Fredrik Anflo, 서성일, 김진영, 남준혁, 권도환, 허정무, 김진휘 그리고 1년간 함께 했던 도경훈까지 모두 부족한 저를 도와주고 항상 친절하게 대해줌은 물론 대학원 생활을 때로는 즐겁게 알차게 때로는 분골쇄신의 정신으로 함께 인내해준 우리 APL의 구성원들에게 정말 크나큰 감사의 인사 전합니다.

또한 지난 2년간 연구가 힘들고 지칠 때면 국궁동아리를 통해 같은 취미를 즐기며 충전의 시간을 함께 해줬던 김형준, 임종규, 이좋은 임원진 들과 동아리의 모든 구성원들에게도 감사의 인사 드립니다.

마지막으로 저를 낳아주시고 이 자리에 오기까지 항상 저를 믿고 응원해주시며 항상 든든한 방패막이 되어 주셨던 부모님과 항상 순수한 마음으로 나를 사랑해주고 응원해준 우리 윤승호 형님에게도 정말 감사 드립니다.

이 모든 분들께 정말 감사드리며, 졸업 후 대한민국을 지키는 강한육군의 일원으로써 그동안 갈고 닦았던 것들을 바탕으로 이들의 감사에 보답하는 마음으로 성실하고 떳떳하게 근무하도록 하겠습니다.

감사합니다.

2023년 2월 6일 윤정훈 올림